Submitted to *Management Science*
manuscript MS-xxxx-xxxx.xx

Designing Stable Coins

Yizhou Cao
FinBook, 148955, Singapore

Min Dai
Department of Mathematics, National University of Singapore, 119076, Singapore

Steven Kou
Questrom School of Business, Boston University, 595 Commonwealth Avenue, Boston, MA 02215, USA

Lewei Li
FinBook, 148955, Singapore

Chen Yang
Department of Systems Engineering and Engineering Management, The Chinese University of Hong Kong, Shatin, N.T., Hong Kong

Stable coins, which are cryptocurrencies pegged to other stable financial assets such as U.S. dollar, are desirable for payments within blockchain networks, whereby being often called the "Holy Grail of cryptocurrency." However, existing cryptocurrencies are too volatile for these purposes. By using the option pricing theory, we design several dual-class structures that offer a fixed income crypto asset (class A coin), a stable coin (class A′ coin) pegged to a traditional currency, and leveraged investment instruments (class B and B′ coins). To understand the impact of the proposed coins on the speculative and non-speculative demands of cryptocurrencies, we study equilibrium with and without the stable coins. Our investigation of the values of stable coins in presence of jump risk and black-swan type events shows the robustness of the design.

Key words: stable coins, fixed income crypto assets, leveraged return crypto assets, smart contracts.
History: This paper was first submitted on May 22, 2018.

1. Introduction

How to create a digital currency was a long-standing open problem for many years, due to two main challenges: First, as people can easily copy music and movie files, how to prevent people from copying digital currency token electronically? Secondly, how to avoid the double spending problem in which a single digital currency token can be spent more than once to settle liabilities? A revolution in FinTech is that the two problems can be solved by using blockchains.

A blockchain is a decentralized (peer to peer) and distributed network that is used to record, after miners' verification, all transactions which can be viewed by every users, thus allowing people to verify and audit transactions in a transparent and inexpensive way. The records cannot be easily altered retroactively. Furthermore, a blockchain confirms with very high probability that each unit of value is transferred only once, solving the double spending problem without a trusted authority[1]. The first blockchain was conceptualized in Nakamoto (2008), and was implemented in 2009 as the core component of the first cryptocurrency, Bitcoin.

Another breakthrough came in late 2013 when Vitalik Buterin extends the idea of Bitcoin to create the Ethereum platform on which people can write smart contracts. This is a very important technology advance, as many types of clerk works, such as public notary, import and export paper works, certain legal and accounting documentations, can be programmed as smart contracts which can be tracked and executed automatically on the Ethereum platform. The cryptocurrency generated and circulated on the Ethereum platform is Ether (with the trading symbol ETH).

Currently, there are over 1000 crytocurrencies traded in exchanges; see, e.g, the list on coinmarketcap.com. Some of them are based on public blockchains, such as Bitcoin and Ether, and others on private blockchains, such as Ripple. In fact, one can buy crytocurrencies from online exchanges or at ATM machines worldwide, just like buying standard financial securities or foreign currencies.

This paper attempts to design stable coins, which are cryptocurrencies pegged to other stable financial assets such as U.S. dollars, by using concepts from the option pricing theory. Stable coins are desirable to be used as public accounting ledgers for payment transactions within blockchain networks, and as crypto money market accounts for asset allocation involving cryptocurrencies.

1.1. Stable Coins

One major characteristic (or drawback) of cryptocurrencies is their extreme volatility. Figure 1 illustrates the price of Ether in U.S. dollars, ETH/USD, from October 1, 2017 to August 31, 2018. During this period, ETH/USD has an annualized return volatility of 107%, which is more than 8 times that of S&P 500 during the same period (13%).

The extremely large volatility means that a cryptocurrency like ETH cannot be used as a reliable means to store value. It is risky to hold the currency even for several days due to this fluctuation. A stable coin is a crypto coin that keeps stable market value against a specific index or asset, most noticeably U.S. dollar. Stable coins are desirable for at least three reasons: (1) They can be used within blockchain systems to settle payments. For example, lawyer or accountants can exchange their stable coins generated by smart contracts automatically for the services they provide within the

[1] Even if an attacker has 10% success probability of finding the next block, in the standard 6 block verification scheme, the chance of the attacker will ever be successful in double spending is only about 0.0005914. Note that the calculation 0.0002428 in Nakamoto (2008) was wrong and was corrected in a recent paper by Grunspan and Perez-Marco (2018).

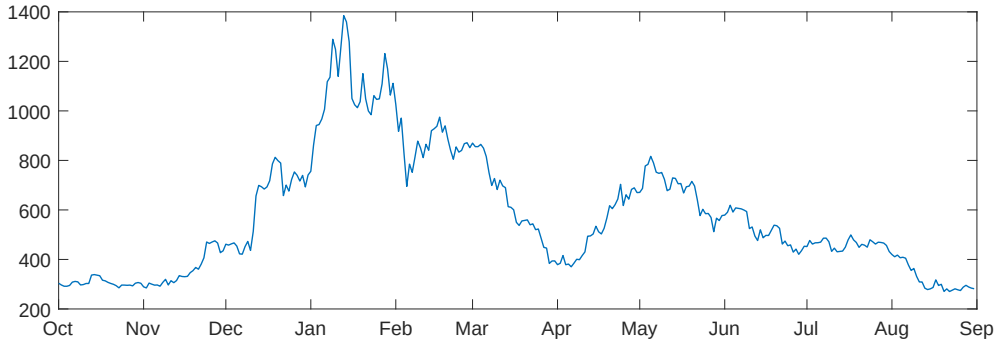

Figure 1 ETH/USD Price from October 1, 2017 to August 31, 2018

system, without being bothered by the exchange fees from a cryptocurrency to U.S. dollar, which can range from 0.7% to 5%. (2) They can be used to form crypto money market accounts, for the purpose of doing asset allocation for hundreds cryptocurrencies. (3) They can be used by miners or other people who provide essential services to maintain blockchain systems to store values, as it may be difficult and expensive for them to convert mined coins into traditional currencies.

However, as we can see, existing cryptocurrencies are too volatile to be served as stable coins. In fact, how to create a good stable coin is called the "Holy Grail of Cryptocurrency" in the media (Forbes, March 12, 2018, Sydney Morning Herald, February 22, 2018, Yahoo Finance, October 14, 2017).

There are four existing types of issuance of stable coins. The first type is an issuance backed by accounts in real assets such as U.S. dollars, gold, oil, etc. More precisely, these stable coins represent claims on the underlying assets. For example, Tether coin is claimed to be backed by USD, with the conversion rate 1 Tether to 1 USD (see Tether (2016)). However, it is very difficult to verify the claim that Tether has enough reserve in U.S. dollar, especially on a daily basis. [2] There are other tokens claimed to link to gold (e.g. Digix, GoldMint, Royal Mint Gold, OzCoinGold, and ONEGRAM), although the claims are also hard to verify.[3]

The second type is the seigniorage shares system, which has automatic adjustment of the quantity of coin supply: When the coin price is too high, new coins are issued; when the coin price is too low, bonds are issued to remove tokens from circulation. A typical example of this type is Basis coin (see Al-Naji (2018)). However, the difficulty of maintaining the right balance of supply and demand of a stable coin is perhaps at the same level of difficulty faced by central banks issuing fiat currencies.

[2] In fact, U.S. regulators issued a subpoena to Tether on December 6, 2017, on whether $2.3 billion of the tokens outstanding are backed by U.S. dollars held in reserve (Bloomberg news, January 31, 2018).

[3] In February 2018, the government of Venezuela issued Petro, a cryptocurrency claimed to be backed by one barrel of oil. Recently in June 2019, Facebook announced Libra (see The Libra Association (2019)), a cryptocurrency backed by a basket of fiat currencies (e.g. USD and the Euro) and low-volatility assets, including bank deposits and government securities), with a targeted date in the first half of 2020.

Indeed, it was announced on Dec. 13, 2018, that the whole Basis coin project will be shutting down.

The third type is an issuance backed by over-collateralized cryptocurrencies with automatic exogenous liquidation. For example, one can generate $100 worth of stable coins by depositing $150 worth of Ether. The collateral will be sold automatically by a smart contract, if the Ether price reaches $110. [4] Examples of this type include the DAI token issued by MakerDAO; see MakerTeam (2017). A main drawback of this type is the relatively large collateral size.

The last type is government-backed stable coins. Besides Venezuela, other countries are considering issuing cryptocurrencies, including Russia and China. Canadian government also did Project Jasper involving the "CAD-coin", in which a Blockchain network is built for domestic interbank payment settlements. There is a virtual currency working group under the Federal Reserve System in U.S., which uses the "Fedcoin" internally. [5] However, a main drawback of issuing stable coins purely by governments is the cost. More precisely, does a government have enough expertise in maintaining a computer system, is a government willing to put enough reserve to back up a stable coin fully, and how does a government control supply and demand of a stable coin in a global anonymous blockchain network?

1.2. Our Contribution

The contribution of this paper is fivefold: (1) We use the option pricing theory to design several dual-class structures that offer entitlements to fixed income stable coins (Class A coins) pegged to a traditional currency as well as leveraged investment opportunities (Class B coins). In contrast to the existing designs whose stability comes from over-collateralization or automatic adjustment of supply, special upward and downward reset barriers are introduced to reduce the credit risk and to maintain the stability of future cash flows. More precisely, due to downward resets, a vanilla A coin behaves like a bond with the collateral amount being reset automatically. The A coin can be further split into additional coins, A′ and B′ , where A′ behaves like a money market account with a very stable cash flow.

(2) We show that the proposed stable coins have very low volatility; indeed the volatility of class A′ coin is so low that it is essentially pegged to the U.S. dollar. Table 1 reports the volatility of ETH, S&P 500 index, Gold price, U.S. Dollar index, class A and A′ coins, respectively.

[4] One can also combine the idea of over-collateralization and seigniorage by issuing more coins if the coin price is too high, and allow people to borrow the coin, which gives borrowers to buy back the coin if the coin price is too low, thus pushing the price higher.

[5] There are several advantages of issuing stable coins by governments. They are cheaper to produce than the cash in bills or coins, and they are never worn out. They can be tracked and taxed automatically by the blockchain technology. They can facilitate statistical works, such as GDP calculation and collecting consumer data. Furthermore, they can simplify legal money transfers inside and outside blockchains. Finally, as pointed out by Bech and Garratt (2017), the main benefit of a retail central bank backed cryptocurrency is that it would have the potential to provide the anonymity of cash.

Table 1 Annualized Volatility of Our Stable Coins versus Common Market Indices

Index	ETH	S&P 500	Gold	US$ Index	Class A Coin	Class A′ Coin
Volatility	107.03%	12.96%	9.55%	5.86%	2.69%	1.14%

Annualized volatility is calculated from October 1, 2017 to August 31, 2018.

(3) We discuss several economic insights of stable coins, such as the potential impact of the introduction of Class A and B coins on the speculative and non-speculative demands of ETH, and on the price sensitivity of ETH; see Section 3.

(4) We show that our design is robust in the sense that the proposal stable coin A′ can maintain its value stability in presence of jump risk (see Section 6), and in the case of Black-Swan type events (when the underlying cryptocurrency suddenly drops close to zero within an extremely short time period), except, for example, when the the underlying asset has a sudden drop more than 60% within a day or within a hour (see Section 2.3).

(5) Technically, in contrast to the standard Black-Scholes partial differential equation (PDE), the pricing equation here is a periodic PDE with a time-dependent upper barrier, which requires a new theoretical derivation of the stochastic representation of the PDE (Theorem 3) and a new numerical procedure (Theorem 4).

1.3. Literature Review

Although our design of stable coins is inspired by dual-purpose funds, it is different from dual-purpose funds in U.S. and China in the aspects shown in Panel A of Table 2. These differences require a different modeling, which is summarized in Panel B of Table 2.

There are many papers and media articles discussed pros and cons of cryptocurrencies. Using cryptocurrencies as a payment method has several benefits. First, as pointed out in Harvey (2016), the core innovation of cryptocurrencies like is the ability to publicly verify ownership, instantly transfer the ownership, and to do that without any trusted intermediary. Thus, cryptocurrencies reduce the cost of transferring ownership. Also, the blockchain technology makes the ledger easy to maintain, reduces the cost of networking (see Catalini and Gans (2016)), and is robust against attackers. The distributed ledger can result in a fast settlement that reduces counterparty risk and improves market quality (see Khapko and Zoican (2018)). Furthermore, since the transaction is recorded to the blockchain anonymously, cryptocurrencies help to protect the privacy of their users. The underlying technology of cryptocurrencies may one day strengthen the menu of electronic payments options, while the use of paper currency is phased out (see Rogoff (2015)).

There are also some criticisms of cryptocurrencies. First, a payment system with cryptocurrencies lacks a key feature, the confidence that one can get his money back if he is not satisfied with the goods he purchased. As pointed out in Grinberg (2011), Bitcoin is unlikely to play an important role

Table 2 Contract and Model Comparison of Our Stable Coins and Dual-Purpose Fund in U.S. and China

Panel A: Contract Comparison					
	Payment Style of A Share	Payment Style of B Share	Reset Barriers	Lifespan	Underlying Asset
Dual-Purpose Fund in U.S.	Dividend	Single payment at wind-up date	No	Finite	Stock/ Stock Index
Dual-Purpose Fund in China	Fixed Income	Payments affect the underlying asset but not the exchange ratio	Yes	Infinite	Stock Index
Our Vanilla A and B Coins	Fixed Income	Payments affect the exchange ratio but not the underlying asset	Yes	Infinite	USD denominated cryptocurrency

Panel B: Model Comparison	
	Pricing Model
Dual-Purpose Fund in U.S. Ingersoll (1976) Jarrow and O'Hara (1989)	Black-Scholes PDE
Dual-Purpose Fund in China Dai et al. (2018)	Periodic PDE, a constant upper barrier
Our Vanilla A and B Coins	Periodic PDE, a time-dependent upper barrier

The dual-purpose funds in U.S. include those studied in Ingersoll (1976) and the prime and scores studied in Jarrow and O'Hara (1989).

in the traditional e-commerce market, since consumers typically do not care about the anonymity that Bitcoin provides; instead, they prefer a currency they are familiar with for most goods and services, and they want fraud protection. Second, Bitcoin does not have identity verification, audit standards, or an investigation system in case something bad happens. For instance, one may lose all his deposit in cryptocurrencies should his password get stolen, and there is no remedy. Furthermore, Blockchain systems are not as trustworthy as they seem to be. Without an intermediary, individuals are responsible for their own security precautions. Finally, it is difficult to value cryptocurrencies like Bitcoin.

Here we want to point out that despite significant drawbacks of cryptocurrencies, it is generally agreed that the blockchain technologies are here to stay. However, blockchain technologies automatically generate cryptocurrencies for the purpose of charging the services provided by the system (such as fees incurred by all programming codes which are run on the Ethereum network), crediting essential services to the system (such as the verification services provided by miners), and of exchanging credits for services. Therefore, cryptocurrencies will not disappear as long as blockchain technologies exist. Thus, designing suitable stable coins is essential for the blockchain system to perform financial functions efficiently and for doing asset allocation across different cryptocurrencies generated by different blockchain systems.

An extensive empirical study of cryptocurrencies is conducted in Chen et al. (2016). Chen et al. (2018) study the pricing of call and put options on cryptocurrencies; here we design nonstandard options with both upper and lower reset barriers, leading to periodic PDEs with a time dependent upper barrier, which requires special numerical algorithm and stochastic representations.

The rest of paper is organized as follows. The design of stable coins is presented in Section 2. An equilibrium analysis is given in Section 3. The valuation of these coins is given in Section 4. Numerical examples under the geometric Brownian motion case are given in Section 5. To capture the jumps in the ETH price, Section 6 extends the geometric Brownian motion framework to a double-exponential jump diffusion framework. Section 7 studies the robustness of our result against a change in the starting date of the simulation. All the technical theorems, propositions and their proofs are given in the appendix.

2. Product Design

In this section, we introduce the detailed design of our stable coin, including its creation/redemption and its cash flow. We also point out several differences between our design, the dual-purpose funds in U.S. and in China, and other stable coins such as DAI.

2.1. Vanilla Class A and B Coins

Our design has a dual-class split structure which, combined with smart contract rules and market arbitrage mechanism, provides the holders of each class with principal-guaranteed fixed incomes and leveraged capital gains, respectively. The Class A Coin behaves like a bond and receives periodical coupon payments. The Class B Coin entitles leveraged participation of the underlying cryptocurrency. Simply put, this split structure means that the holders of Class B coins borrow capital from the holders of Class A coins and invest in a volatile cryptocurrency. Furthermore, a set of upward and downward reset clauses is imposed, where downward resets reduce default risk of Class B to protect Class A, and upward resets ensure a minimum leverage ratio of Class B to make Class B attractive to leverage investors. Furthermore, both Class A and B shares can be traded on exchanges.

For illustration we choose ETH as the underlying cryptocurrency, and the initial leverage ratio is set to 2.[6][7] Class A and B coins can be created by depositing ETH shares to a custodian smart

[6] The design of a contract with a general initial leverage ratio is discussed in Appendix A.

[7] Several remarks about the practical implementations: (1) The underlying can be a diversified portfolio of digital assets, including fiat-backed stablecoins. However, there are two challenges: (a) Currently, major cryptocurrencies (e.g. BitCoin, Ripple, LiteCoin) can only be transacted on their respective blockchains, and cannot be handled by Ethereum smart contracts; cross-chain projects are still under-developed. (b) A dual-class token on a portfolio of digital assets might be classified as a security in certain countries. (2) One can also use ERC20 tokens on the Ethereum blockchain as the underlying basket. However, these ERC20 tokens are not as popular as the ETH. (3) In the future it might be possible to run our system on a government-run permissioned blockchain, if it gains mass adoption. A permissioned blockchain could yield higher throughput and shorter blocktimes, which may significantly reduce the time required for resets and support many more accounts.

contract.[8] Upon receiving two shares of underlying ETH at time t, the custodian contract will return to the depositor $\beta_t P_0$ of Class A and Class B coins each, where P_0 is the initial price of underlying ETH in USD at the inception of the coins ($t = 0$), and β_t is the time-t conversion factor. We set $\beta_0 = 1$, which means that two shares of ETH can initially exchange for P_0 shares of Class A and Class B each. The conversion factor β_t changes only on upward/downward resets or regular payout dates, and the change rule will be introduced later. To withdraw ETH at time t, holders of Class A and Class B coins can send, e.g., $\beta_t P_0$ shares of Class A and Class B coins each to the Custodian contract, then the contract will deduct the same amount of Class A and Class B coins, and return to the sender two ETHs. For instance, if the initial ETH/USD price is 500 and $\beta_t = 1$, then two shares of ETH can create 500 shares of Class A coins and Class B coins each, and 500 shares of Class A and B coins each can be redeemed into two shares of ETH. Figure 2 illustrates this split structure.

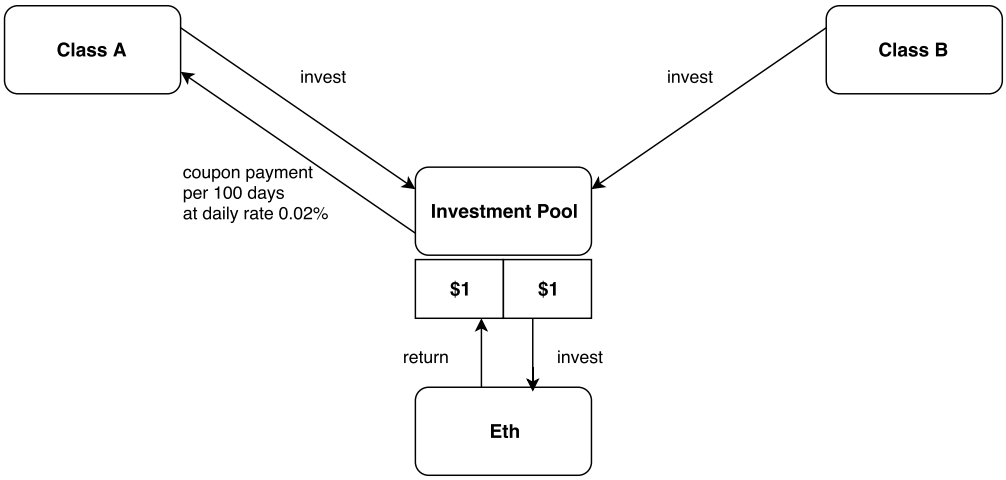

Figure 2 Class A and B, Initial Split. At time t, one share of Class A and B each invests $1 in ETH. The initial ETH price is $P_0 = \$500$, and the prevailing conversion factor $\beta_t = 1$. So two shares of ETH exchange for 500 shares of Class A coins and 500 shares of Class B coins.

To describe the cash flow of Class A and B coins, we introduce the net asset dollar values of Class A and B coins, V_A and V_B. Thanks to the exchange between ETH and Class A/B coins, the following parity relation holds at any time:

$$V_A^t + V_B^t = \frac{2P_t}{\beta_t P_0}, \tag{1}$$

[8] A custodian smart contract can perform multiple tasks that facilitate key mechanism of the system, including: creation and redemption of the stable coin, safekeeping the underlying digital assets (e.g. ETH), calculation of stable coins' net values, and execution of reset events. The deposited underlying cryptocurrency is kept by the custodian smart contract. Any user or member of the public can verify the collateral and coins issued through third party applications such as Etherscan.io. When forking on the Ethereum blockchain occurs, the custodian smart contract will automatically switch to the mainstream fork; more precisely, the contract will maintain price fixing and all the relevant event triggering mechanism on the mainstream chain.

where P_t is the prevailing price of underlying ETH in USD. The net asset value of Class A coins at time t is defined as

$$V_A^t = 1 + R \cdot v_t, \tag{2}$$

where R is the *daily* coupon rate, and v_t is the number of days from the inception, last reset, or last regular coupon payout date, whichever is most recent. The above design ensures that the initial net asset values of Class A and B coins are both equal to one dollar.

2.1.1. Regular Payout Assume regular coupons are paid every T days. When $v_{t-} = T$, i.e., $V_A^{t-} = 1 + RT$, a regular payout is triggered, then the holder of each Class A coin receives payment with dollar value RT,[9] and the net asset value of Class A resets to \$1, namely, $V_A^{t+} = 1$. Since no cash flow occurs for Class B coin upon regular payout, the net asset value of Class B remains unchanged, that is, $V_B^{t-} = V_B^{t+}$. Noting that the parity relation (1) always holds across regular payout, we deduce that the conversion factor β experiences a jump upon regular payout:

$$\beta_{t+} = \frac{2P_t}{2P_t - \beta_{t-} P_0 RT} \beta_{t-}.$$

For instance, assuming $R = 0.02\%$, $T = 100$, and $P_0 = \$500$, a regular coupon payout occurs at time t when $P_t = \$450$ and $\beta_{t-} = 1$, then Class A receives \$0.02 coupon payment, and the conversion ratio is reset to $\beta_{t+} = 1.011$, which indicates that two shares of ETH can exchange for 505.62 shares of Class A and 505.62 shares of Class B after the regular payout. This is illustrated in Figure 3.

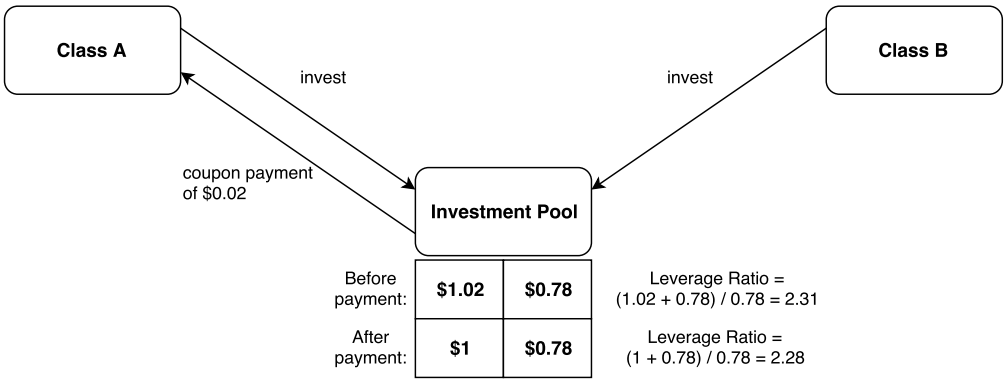

Figure 3 Class A and B, Regular Payout. After 100 days, the ETH price drops to \$450, so that total investment of one Class A coin and one Class B coin becomes \$1.8, within which \$1.02 belongs to Class A. A regular payout takes place, and Class A receives \$0.02 coupon payment. New exchange ratio: 2 shares of ETH now correspond to 505.62 ($= 500 \times \frac{2\times 450}{2\times 450 - 500 * 0.02}$) shares of Class A and 505.62 shares of Class B, yielding $\beta_{t+} = 1.011$.

[9] Payments are made in the form of underlying ETH from the Custodian contract. For instance, upon regular payout, the holder of each Class A coin receives underlying ETH with amount $\frac{RT}{P_t}$.

2.1.2. Upward Reset An upward reset is triggered when the net asset value of Class B coins reaches the predetermined upper bound, denoted by $\mathcal{H}_u$. On an upward reset time t, net asset value of both classes resets to 1 USD, Class A and B's holders will receive payments of value $V_A^t - 1$ and $V_B^t - 1$, respectively, and the conversion factor β_{t+} is reset to P_t/P_0 so that after the upward reset two shares of ETH can exchange for P_t share of class A and B. For instance, as illustrated in Figure 4, after another 50 days, the ETH price grows to \$760.96, so the net asset value of the Class B grows to $\mathcal{H}_u \equiv \$2$, triggering an upward reset. The holders of Class A and B receive payments with amount \$0.01 and \$1, respectively. Two shares of ETH now correspond to 760.96 shares of Class A and 760.96 shares of Class B, yielding $\beta_{t+} = 1.52$.

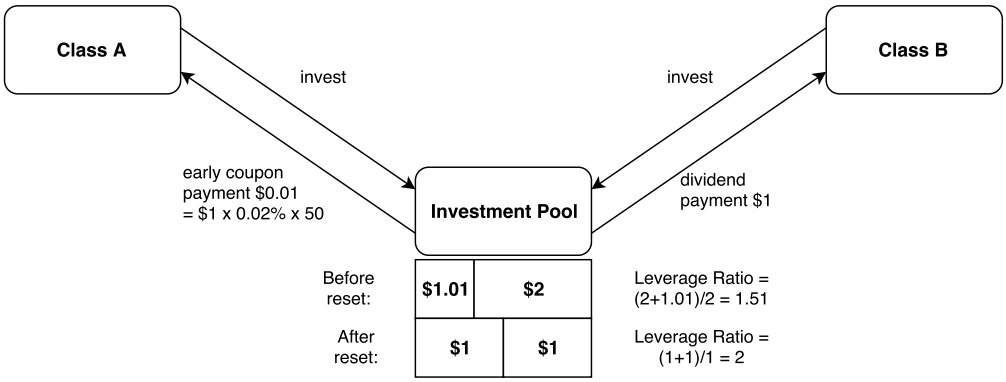

Figure 4 Class A and B, Upward Reset. After 50 days, the ETH price grows to \$760.96, and Class B NAV grows to \$2, triggering an upward reset. Class A NAV equals \$1.01, where \$0.01 is 50-day accrued coupon. On this date, Class A receives \$0.01 coupon payment, and Class B receives \$1 dividend payment. New exchange ratio: 2 shares of ETH now correspond to 760.96 shares of Class A and 760.96 shares of Class B, yielding $\beta_{t+} = 760.96/500 = 1.52$.

2.1.3. Downward Reset A downward reset is triggered when the net asset value of Class B coins reaches the predetermined lower bound, denoted by $\mathcal{H}_d$, On a downward reset time t, Class A holders receive a payment with dollar value $V_A^t - \mathcal{H}_d$, and $1/\mathcal{H}_d$ shares of Class A and B are merged into one share of Class A and B, respectively, so that the net asset value of both classes resets to \$1. The conversion factor β_{t+} resets to P_t/P_0, that is, two ETHs can exchange for P_t shares of Class A and B after the reset. For instance, as illustrated in Figure 5, after another 50 days, the ETH price drops to \$479.40, so that the net asset value of Class B drops to $\mathcal{H}_d \equiv \$0.25$, triggering a downward reset. Class A receives \$0.01 coupon payment and \$0.75 principal payback, and then both classes undergo a 4:1 merger. Two shares of ETH now correspond to 479.40 shares of Class A and 479.40 shares of Class B, yielding $\beta_{t+} = 479.40/500 = 0.96$.

Under a black swan event, the net asset value of Class B coins V_B^t is likely lower than $\mathcal{H}_d$ or even becomes negative upon downward reset. In the case of $V_B^t > 0$, we can simply replace $\mathcal{H}_d$ by V_B^t for

the above description of cash flow and operations on downward reset. If $V_B^t \leq 0$, then both classes are fully liquidated, the holders of Class B receive nothing, and the holders of Class A receive the payment $V_A^t - |V_B^t|$.

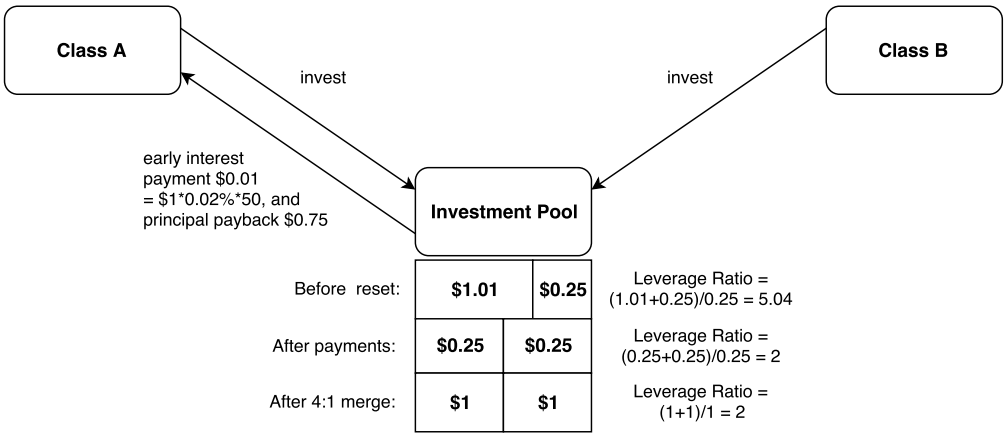

Figure 5 Class A and B, Downward Reset. After another 50 days, the ETH price drops to $479.40, and Class B NAV drops to $0.25, triggering a downward reset. Again, Class A NAV equals $1.01, where $0.01 is 50-day accrued coupon. On this date, Class A receives $0.01 coupon payment, as well as $0.75 principal payback. Then, Class A and B each undergo a 4:1 merger, so that both have NAV equal to $1. New exchange ratio: 2 shares of ETH now correspond to 479.40 shares of Class A and 479.40 shares of Class B, yielding $\beta_{t+} = 0.96$.

Note that, the net asset values used in the triggering condition of the reset clauses can be computed automatically without using any models. Thus, in practice, the upward and downward reset mechanisms can be implemented via a smart contract on the Ethereum blockchain, and they are *automatically* triggered and executed in real time when the net asset value of Class A or B satisfies the triggering conditions specified above.

Since Class A and B shares are traded on exchanges, besides their net asset values, they also have market/model prices, which will be studied in Section 4. *No arbitrage* implies that the market prices of Class A and B coins also satisfy the parity relation:

$$W_A^t + W_B^t = \frac{2P_t}{\beta_t P_0},$$

where W_A and W_B are the market prices of the Class A and B coins, respectively. This has an interesting implication: Suppose the demand of Class B coins is low, then the market value of Class B coins would be low, and the above parity relation implies that the market value of the Class A coins would be high.

The above split design is related to tranching technique in securitization (e.g. collateralised debt obligations). What is new here is the carefully designed reset mechanism. Without this reset mechanism, tranching alone is not enough for controlling the risk of Class A coins (and A′ to be introduced

in Section 2.2), especially when the underlying value becomes low. For example, the downward reset mechanism reduces the risk when the underlying price is low, by partially paying back the principal. As a result, upon a reset, the tranches are restructured based on their value before the reset and a pre-specified set of rules.

The incorporation of the reset mechanism requires a delicate treatment even for a single tranche; one cannot apply existing financial engineering results to solve for the value of each tranche. Indeed, the future cash flow of Class A coins is periodic and path-dependent on the underlying value, resulting in a periodic PDE rather than the standard Black-Scholes PDE. To our best knowledge, this type of cash flow has not been extensively discussed in securitization literature. In Section 4, we derive a rigorous PDE characterization of the fair value of this type of cash flow under a geometric Brownian motion assumption, enabling numerical solution via PDE that is more efficient than the Monte Carlo method based on the cash flow.

Class A coin behaves like a bond. Although Class A has a fixed coupon rate and its coupon payment is periodic and protected by the downward resets, its value is still volatile on non-coupon dates. This is because the coupon rate is usually higher than the risk-free rate, and on a downward reset, a portion of Class A coin will be liquidated, then the holder of Class A will lose high coupons that would be generated from this portion. Therefore, a potential downward reset will make the price of Class A volatile. In the following, we will propose one more type of stable coins: A′ coins.

2.2. Class A′ and B′ Coins

This extension splits Class A into two sub-classes: Class A′ and B′ . Both classes invest in Class A coins. At any time, two Class A coins can be split into one Class A′ coin and one Class B′ coin. Conversely, one Class A′ coin and one B′ coin can be merged into two Class A coins. The split structure for Class A′ and B′ resembles that for Class A and B: Class B′ borrows money from Class A′ at the rate R' to invest in Class A. Here R' is set to be close to the risk-free rate r, whereas the rate R for Class A is generally much higher.

Class A′ and B′ resets *when and only when* Class A resets or gets regular payout. Class A′ gets coupon at the rate R' on regular payouts, upward and downward reset (provided that the net asset value of Class B is positive then), and Class B′ gets coupon at the rate $2R - R'$ on upward reset. On downward resets, each share of both Class A′ and B′ is reduced to $(V_B^t)^+$ share, and Class A′ gets the value of the liquidated shares (i.e., $1 - (V_B^t)^+$ shares). In the extreme case where $V_B^t \leq 0$, then both Class A′ and B′ are fully liquidated, and A′ receives its full net asset value $1 + R'v_t$, or the remaining total asset for A′ and B′ , $2(1 + Rv_t - |V_B^t|)$, whichever is smaller. Using the same example as in Section 2.1, Figure 6 illustrates the cash flow of Class A′ and B′ coins.

As we will see later, Class A′ behaves like a money market account, except in the extreme case in which the underlying asset suddenly suffers huge losses in a very short period (e.g. a sudden 60% or

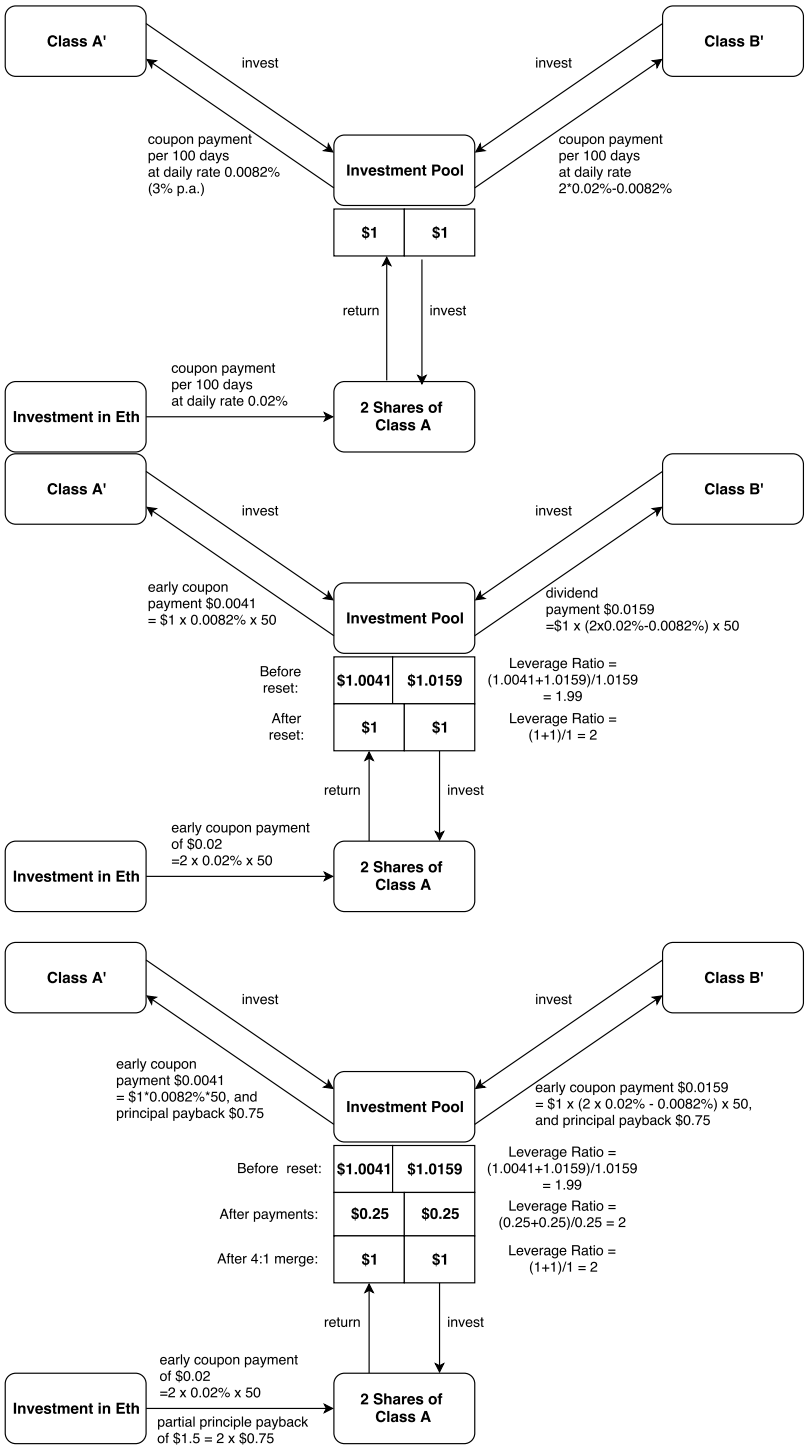

Figure 6 Top Figure: **What happens to Class A′ on a regular payout date of A. On regular payout dates for Class A (per 100 days), 2 shares of A receive coupon payment $0.04, i.e. at daily rate 0.02%. $0.0082 is paid to A′ and $0.0318 to B′ .** Middle Figure: **Upward Reset of Class A′ . After 50 days, Class B's net asset value grows to $2, triggering an upward reset.** Bottom Figure: **Downward Reset of Class B′ . After another 50 days, Class B's net asset value drops to $0.25, triggering a downward reset.**

more drop within a day or within a hour). Here is an intuition on this. The stability of Class A′ coin price comes from its stable future cash-flow, as Class A, B and B′ coins act like buffers for Class A′ . Indeed, the volatility of ETH spreads to Class A′ coin only via the timing of coupons (on regular payment or upward resets) or the partial payback on principal (on downward reset dates). Since the accrued amount of coupon grows linearly with respect to time, and the coupon is expected to be paid at least once per 100 days, the timing of the coupon payment does not cause a large volatility on Class A′ nominal price; the volatility of the total return (taking into account the coupon) is even smaller. By setting the coupon rate to be close to the risk-free rate, the value of future coupons is close to 1. Therefore, on a downward reset date, the partial payback of principal (at book value) also does not cause large impact to the cash flow.

2.3. A Model-Free Bound for Black Swan Events

Despite the protection provided by the downward reset mechanism, when there is a sudden drop in ETH value Class A and A′ still can take a loss, i.e., losing part of the accrued coupon or even the principal. Here we give a model-free bound on how large the jump in ETH should be to trigger such a loss.

We take Class A′ as an example. According to the contract design, Class A′ takes a loss if and only if the net asset value of Class B becomes negative, i.e. $V_B^t \le 0$, and the payment to Class A′ (i.e. the net asset value of 2 shares of Class A) is lower than the net asset value of Class A′, i.e. $2(1+Rv_t-|V_B^t|) < 1+R'v_t$, on a downward reset time t. These two conditions are equivalent to $V_B^t \le 0$ and $V_B^t < \frac{R'v_t-1}{2} - Rv_t$. In other words, assuming $(R'-2R)T-1 \le 0$, Class A′ takes a loss if and only if V_B *jumps* from $\mathcal{H}_d$ or above to a negative level below $\frac{R'v_t-1}{2} - Rv_t$ (if V_B drops downward without a jump, a downward reset will be triggered instead and Class A′ will not take a loss). This further means that, assuming $(R'-2R)T-1 \le 0$, to incur a loss in Class A′ coins, the ETH price must have a single-day (negative) return lower than $\frac{1}{2}\frac{R'v_t+1}{Rv_t+1+\mathcal{H}_d} - 1$.

In our design example, we set $R = 0.02\%$ (7.3% p.a.), $R' = 0.0082\%$ (3% p.a.), $\mathcal{H}_u = 2$, $\mathcal{H}_d = 0.25$, $r = 0.0082\%$ (3% p.a.), $T = 100$. With these contract parameters, we have

$$\max_{0\le v\le T} \frac{1}{2}\frac{R'v+1}{Rv+1+\mathcal{H}_d} - 1 = -60\%,$$

meaning that unless there is a sudden downward jump of more than -60% between the monitoring time points, Class A′ will not take a loss. In comparison, the historical maximal single-day loss of ETH is recorded at -60% on its second trading day (8 Aug 2015), at which time the market was yet to be familiar with it. The maximum single-day loss thereafter is only -26.67% recorded on 18 Jun 2016 when the DAO hacking occurred, which is not large enough to trigger a loss in Class A′ coin. In a practical implementation, the ETH price can be monitored at a higher frequency, e.g. hourly.

Therefore, Class A′ would take a loss only when ETH price jumps downward at this magnitude or more within an hour, which is even less likely.

In comparison, the DAI token starts to take loss when its total collateral value suddenly drops from 150% of the DAI value to below 100%, i.e. with a -33% downward jump. Therefore, Class A′ coin may withstand a larger sudden downward jump in ETH than the DAI token does. By further splitting Class A′ to get A″, the resulting new stable coin A″ can withstand even larger downward jumps before taking any loss.

2.4. A Contract Design with the Subsidy from Class A Coins to Class B Coins

One might worry about the demand of Class B coins, as they are leveraged products. Of course, if the demand of Class B coins is low, then the price of Class A coins may be overpriced. If one wants to provide extra incentive for investors to hold Class B coins, one can modify the contract so that Class B coin holders receive coupon payment from Class A coins, as described below.

The modified contract for Class A, B, A′ and B′ differs from the one introduced in Section 2.1 and 2.2 only in the payoff on downward resets. Specifically, on a downward reset time t, if $V_B^t \geq 0$, Class A holders receive a payment with dollar value $V_A^t - (V_B^t)^+ - (V_A^t - 1)\frac{\tilde{R}}{R}$,[10] Class B holders receive a payment with dollar value $(V_A^t - 1)\frac{\tilde{R}}{R}$, and each share of Class A and B is reduced to $(V_B^t)^+$ share of Class A and B, respectively. Class A′ holders still receive accrued coupon payment $R'v_t$ plus the value $1-(V_B^t)^+$ of the liquidated shares. Class B′ holders receive coupon payment $(2R-R')v_t$ plus the value $1-(V_B^t)^+$, *minus* $2(V_A^t-1)\frac{\tilde{R}}{R}$; and then each share of both Class A′ and B′ is reduced to $(V_B)^+$ share.

In extreme events the net asset value of Class B can jump to a negative value, that is $V_B^t \leq 0$. In this case, all four shares are fully liquidated. Class A receives a payment with dollar value $(V_A^t - |V_B^t| - (V_A^t-1)\frac{\tilde{R}}{R})^+$, and Class B receives $\min\{(V_A^t-1)\frac{\tilde{R}}{R}, V_A^t - |V_B^t|\}$. That is, Class B receives the full subsidy if Class A can still cover it; otherwise, Class B receives the remaining net asset value of Class A, if any. Class A′ receives its full asset value $1+R'v_t$, or the remaining total asset for A′ and B′ , $2(V_A^t - |V_B^t| - (V_A^t-1)\frac{\tilde{R}}{R})^+$, whichever is smaller. Finally, Class B′ receives the remaining total asset value for A′ and B′ minus the payment to A′ .

In this case we can also get a model-free bound on how large the jump in ETH should be to trigger such a loss. Class A′ will take a loss when and only when $V_B^t \leq 0$ and $2(V_A^t - |V_B^t| - (V_A^t-1)\frac{\tilde{R}}{R})^+ < 1+R'v_t$, i.e. the payment to Class A′ is lower than the net asset value of Class A′ , on a downward reset date. A similar argument as in Section 2.3 shows that, assuming $(R'-2R+2\tilde{R})T-1 \leq 0$, this

[10] This equals $V_A^t - (V_B^t)^+ - \tilde{R}v_t$ (recall that v_t is the time from the inception, last reset or regular coupon payout, as defined in (19)). We require $0 \leq \tilde{R} \leq \frac{1-\mathcal{H}_d}{2T} + R - \frac{R'}{2}$ to ensure that Class A, B, A′ and B′ all receive nonnegative payments in normal stances where $V_B \geq 0$. Under the contract parameter given in Section 2.3, this means $0 \leq \tilde{R} \leq 0.387\%$ (142.67% p.a.).

will happen only when the ETH price has a sudden (negative) return lower than $\frac{1}{2}\frac{R'v_t+1+2\tilde{R}v_t}{Rv_t+1+\mathcal{H}_d}-1$. Using the contract parameter as in Section 2.3 as well as $\tilde{R}=0.0274\%$ (10% p.a.), we have

$$\max_{0\le v\le T}\frac{1}{2}\frac{R'v_t+1+2\tilde{R}v_t}{Rv_t+1+\mathcal{H}_d}-1=-52.4\%,$$

meaning that unless there is a sudden downward jump of more than -52.4%, Class A$'$ will not take a loss.

2.5. Differences between Our Design and the Design of the Dual-Purpose Fund

There are four main differences between our stable coin with dual-purpose funds in China. First, in China a dual-purpose fund and its underlying fund share the same fund managers, hence the fund managers re-scale the value of the underlying fund upon upward and downward resets and regular payouts, in order to easily ensure the no arbitrage parity relation between the dual-purpose fund and the underlying fund. Since we cannot change the underlying ETH price, we instead change the exchange ratio of the shares between the underlying ETH and Class A and B coins in our case, to maintain no-arbitrage across upward and downward resets and regular payouts.

Second, for the dual-purpose funds, the upward reset is triggered by the underlying up-crossing $\mathcal{H}_u$ while the downward reset is triggered by the net asset value of B share down-crossing $\mathcal{H}_d$. In contrast, for our stable coin, the triggering conditions of both upward and downward resets are all based on the net asset value of Class B coins. This is because unlike the re-scaled underlying fund value in China, the underlying ETH price is not so appropriate as the net asset value of Class B to measure the leverage ratio of Class B.

Third, the underlying funds of Chinese dual-purpose funds incur management fees, whereas the underlying ETH does not. Finally, the periodic payout of dual-purpose fund is annually at a fixed date (e.g. first trading day of each year), while the periodic payout of our Class A coins happens when a pre-specified time has passed from the last reset or payout event, which reduces the frequency of payouts, making the coins more stable.

2.6. Differences between Our Design and the Design of the DAI token

An issue with real asset backed stable coins is: how to verify the deposit account in real time? In other words, instead of asking an accountant to check the value in deposit account every few months, can an investor see the deposit value any time in a timely fashion? There are two ways to solve this issue. One is an issuance backed by over-collateralized cryptocurrencies with automatic exogenous liquidation, such as in the DAI token. In this case, one can see the market value of the deposit account, which is in ETH, instantaneously as one wishes. The second one is what we propose here to create stable coins by using tranches with carefully designed resets.

The main difference between the DAI design and our design is that the DAI design needs a relatively large collateral size, while our design does not require this. More precisely, to generate \$100 worth of stable coins the DAI design needs to deposit \$150 worth of ETH. For our design, the firm mainly serves to do the conversion, with all the A, B, A′ and B′ tokens traded outside the firm and in exchanges. In particular, the main function of the firm is to give a person A and B (A′ and B′ tokens) tokens if the person brings the ETH (Class A token) to convert. This way the capital requirement of our design may be much less, compared to that of the DAI token.

There are also two technical differences. First, they are different financial instruments. By design, the DAI token is an instrument pegged to US dollar. It maintains its level by the promise of one dollar during the settlement, and an auto-liquidation mechanism when the collateral-to-debt ratio drops below certain threshold (150% at present). In contrast, Class A and A′ coins are more like a bond and a money market account, respectively. The stability of their values comes from the stability of their future cash flows. The volatility of the underlying ETH spreads to Class A and A′ coin via the timing of coupons or the partial payback on principal (on downward resets); numerical examples in Section 5 demonstrate that their volatility is indeed small, especially for Class A′ coin which is almost pegged to US dollar. Secondly, compared with the DAI token, our design has an additional feature of tranching with carefully chosen reset barriers to reduce the risk and to enhance stability. As illustrated in Section 2.2, Class A coins can be split into A′ and B′ coins. Since Class A′ coins are backed by both Class B and B′ coins, they are likely more stable and more robust to Black Swan events than Class A coins, as will be demonstrated by the numerical examples in Section 5. Based on the same idea, one can further split Class A′ to get an even stabler type of coins, so on and so forth, if one wishes.

It should be noted that the tranche structure in our design is not standard; for example, when the value of Class B tranche falls below the lower threshold, triggering the downward reset, the remaining tranches are restructured and partially payback. This adds an additional layer of protection.

3. Economic Insights

In this section, we discuss the potential impact of introducing Class A and B coins on the speculative and non-speculative demands of ETH, and on the price equilibrium and price sensitivity of ETH, by building equilibrium models.

3.1. Monetary Equilibrium with ETH Only

Our equilibrium model extends the classical framework of Barro (1979) by incorporating the factor of investment attractiveness of ETH as in Ciaian et al. (2016) and by tailoring to the special structure of Class A and B coins. The total ETH supply is taken as $M^S = P^E E$, where E is the total stock of ETH, and P^E is the price of ETH denominated by USD. The demand of ETH as medium of

exchange is modelled in the same way as Barro (1979): $M^D_{Exchange} = \frac{PG}{V^E}$, where P is the price level of goods and services, G is the size of cryptocurrency economy, and V^E is the velocity of ETH circulation. The demand of ETH for speculation depends on its current price level P^E, and its investment attractiveness a (c.f. Ciaian et al. (2016)), i.e. $M^D_{Speculation} = f(P^E, a)$.

ASSUMPTION 1: The function f is assumed to satisfy: (i) $f \geq 0$ and is twice differentiable in P^E and differentiable in a; (ii) for a given P^E, f is increasing in a; (iii) for a given a, the marginal demand $\frac{\partial f}{\partial P^E}$ is negative, increasing in P^E, and increases to 0 when P^E goes to infinity; and (iv) $f(\cdot, 0) = 0$.

In the above assumption, the first item is a technical condition to establish equilibrium. The second one means that the demand of ETH is higher if it has a greater attractiveness (e.g. from news). The third one is typical for the demand function: the demand of ETH is lower if its price is higher, since it is too risky for investment. On the other hand, when the price is very high, the marginal decrease in demand with respect to price becomes lower and eventually vanishes. Finally, the last item says that if there is no speculative attractiveness of ETH, its speculative demand is zero.

The total demand of ETH is then $M^D = M^D_{Exchange} + M^D_{Speculation}$. In equilibrium, the supply of ETH M^S equals its demand M^D. Therefore, a combination of the equations above gives

$$f(P^E, a) + \frac{PG}{V^E} = P^E E. \tag{3}$$

THEOREM 1. *With $E, P, G, V^E > 0$ and $a \geq 0$, under Assumption 1, there exists a unique positive equilibrium price of ETH $P^{E,*}$ satisfying* (3)*. Moreover, (i) $P^{E,*}$ is increasing in PG and decreasing in V^E, E; (ii) $P^{E,*}$ is increasing in a.*

3.2. Monetary Equilibrium with ETH and Class A and B

Now we add Class A and B coins into the previous equilibrium model. We make the following assumption on the split of A and B.

ASSUMPTION 2: We assume that ETH can be converted into Class A and B with equal value.

Supply of ETH. Denote q as the fraction of ETH converted to Class A and B, so that the total ETH supply is reduced to $M^S = P^E E(1-q)$. Denote by $f(P^E, a)$ the speculators' demand of ETH and B, who want to invest γ_2 fraction in B and the remaining in ETH. Therefore, the demand of B is $D^B = \gamma_2 f(P^E, a)$. Since one unit of ETH can be converted into B of USD value $0.5P^E$, the demanded stock of ETH that needs to be converted is $\frac{D^B}{0.5P^E}$. The influence of this demand on the fraction of ETH converted is expressed as $q = g\left(\frac{D^B}{0.5P^E}\right)$, where g satisfies the following assumption.

ASSUMPTION 3: We assume that (i) g is concave and increasing, (ii) $g(0) = 0$ and $g'(0) = 1/E$, and (iii) $g(+\infty) = 1$.

In this assumption, part (i) says that the proportion of ETH converted, q, increases with the demands stock of ETH to be converted; part (ii) means that no stable coins will be created if there

is no demand for it, and the demand of B will be completely met initially when there is no existing B; part (iii) indicates that the fraction of ETH converted to stable coins is limited by 1. The total supply of A (or equivalently B) is then $0.5P^E E \cdot g\left(\frac{D^B}{0.5P^E}\right)$.

Demand of ETH. The total demand consists of five parts: (1) speculative demand of ETH; (2) speculative demand of A (e.g. for asset allocation); (3) speculative demand of B; (4) real economy demand of A (e.g. as medium of exchange); and (5) real economy demand of ETH (e.g. as payment method for services over Ethereum network). Note that B does not have a real economy demand. Within the total real crypto-economy PG (for ETH and A), we assume that $\gamma_1\gamma_2 PG$ goes to A and the remaining goes to ETH. Here $\gamma_1\gamma_2 < 1$, since ETH is always needed for payment of certain services on the Ethereum network. γ_1 is typically very small (as we expect that the market share of A may be small compared to that of ETH). Table 3 describes the proportions of different types of demand.

Table 3 Demand Proportion of the Whole Market

	Real Economy Demand	Speculative Demand
ETH	$(1-\gamma_1\gamma_2)\frac{PG}{V^E}$	$(1-\gamma_2)f(P^E,a)+\gamma_1\gamma_2\frac{PG}{V^E}-0.5P^E Eg\left(\frac{\gamma_2 f(P^E,a)}{0.5P^E}\right)$
A	$\gamma_1\gamma_2\frac{PG}{V^E}$	$0.5P^E Eg\left(\frac{\gamma_2 f(P^E,a)}{0.5P^E}\right)-\gamma_1\gamma_2\frac{PG}{V^E}$
B	0	$\gamma_2 f(P^E,a)$
Total	$\frac{PG}{V^E}$	$f(P^E,a)$

After the introduction of A+B, the total real economy demand and speculative demand are reallocated, but the total demand within each type remains unchanged. The total demands of A and B are equal. Within the real economy demand, $\gamma_1\gamma_2\frac{PG}{V^E}$ belongs to A, where $\gamma_1 > 0$ is small. Within the total speculative demand, γ_2 fraction goes to B. Speculative demand of A refers to the demand for asset allocation purpose.

Equilibrium with ETH and Class A and B. In equilibrium, the total demand of ETH (given as the summation of the first row of Table 3) equals to the total supply, meaning

$$(1-\gamma_2)f(P^E,a)+\frac{PG}{V^E}=P^E E\left(1-0.5g\left(\frac{\gamma_2 f(P^E,a)}{0.5P^E}\right)\right). \tag{4}$$

THEOREM 2. *With $E,P,G,V^E>0$, $a\geq 0$, $0\leq\gamma_1\leq 1$, and $0<\gamma_2\leq 0.5$, under Assumptions 1–3, there exists a unique positive equilibrium price of ETH, $P^{E,*}$ satisfying* (4)*. Moreover, $P^{E,*}$ is increasing in a.*

3.3. Numerical Illustrations

The following numerical results present the potential impact of the introduction of stable coins on the ETH economy. To illustrate, we assume that $f(P^E,a)=k\cdot(1+P^E)^{-\eta_1}\cdot a^{\eta_2}$ with $\eta_1>0, 0<\eta_2<1$, and $g=\frac{x}{E+x}$. All results are calculated under the following default parameters:

$$V^E=0.2, P=G=1, a=k=100, \eta_1=1, \eta_2=0.5, E=0.1, \gamma_1=0.05, \gamma_2=0.5.$$

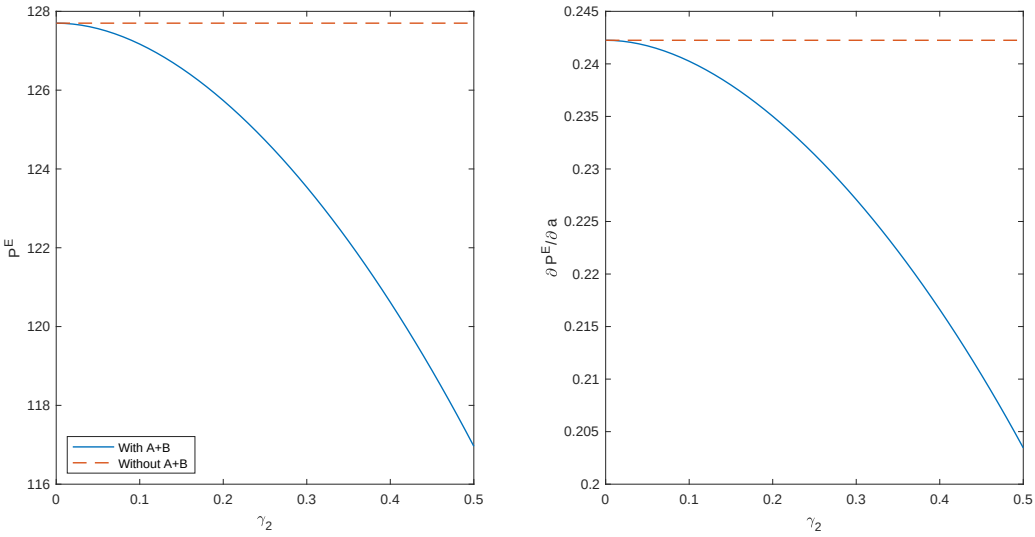

Figure 7 The impact of speculative demand in Class B on the equilibrium ETH price (left panel) and on the sensitivity of ETH price to attractiveness (right panel). Default parameters: $V^E = 0.2$, $P = G = 1$, $a = k = 100$, $\eta_1 = 1$, $\eta_2 = 0.5$, $E = 0.1$, $\gamma_1 = 0.05$. γ_2 **is the fraction of speculators' demand in B.** $\gamma_1\gamma_2$ **is the fraction of crypto-economy using A. The figures show that both the ETH price and its sensitivity to attractiveness decrease as the fraction of speculators' demand in B increases.**

Figure 7 shows the impact of introducing Class A and B on the equilibrium ETH price and its sensitivity to attractiveness, for $\gamma_2 \in [0, 0.5]$.[11] This figure suggests that introducing Class A and B can help stabilize ETH by reducing its price and reducing ts sensitivity to attractiveness (e.g. making it less fluctuate with respect to news). Furthermore, ETH becomes more stable if a larger fraction of speculators uses Class B for speculation.

Figure 8 shows the equilibrium composition of cryptocurrency market after the introduction of Class A and B. As the fraction of speculative of Class B increases (i.e. γ_2 increases from 0 to 0.5), the fraction of speculative ETH use decreases, while the speculative use of Class B and asset allocation use of Class A increase. The non-speculative use of Class A also increases, although the fraction remains small even for large γ_2.

To see why the introduction of Class A and B can help stabilize the ETH price, Figure 9 shows the demand and supply curve before and after introducing Class A and B, with the initial equilibrium price of ETH without A and B being 100. As expected, the introduction of Class A and B reduces both the demand and supply of ETH. Furthermore, the percentage reduction in demand is larger

[11] We take $\gamma_2 \leq 0.5$ which means that most speculators still prefer ETH over B. to make sure ETH has a positive speculative demand. Indeed, as γ_2 increases to 1, ETH's speculative demand can become negative (c.f. Table 3), since an increase in B's speculative demand also increases A's demand. By assuming $\gamma_2 \leq 0.5$, we have $(1-\gamma_2)f(P^E, a) - 0.5P^E Eg\left(\frac{\gamma_2 f(P^E,a)}{0.5P^E}\right) \geq (1-2\gamma_2)f(P^E, a) \geq 0$, thanks to Assumption 3. Also, γ_2 is small in practice, since most investors still prefer ETH for speculative purpose.

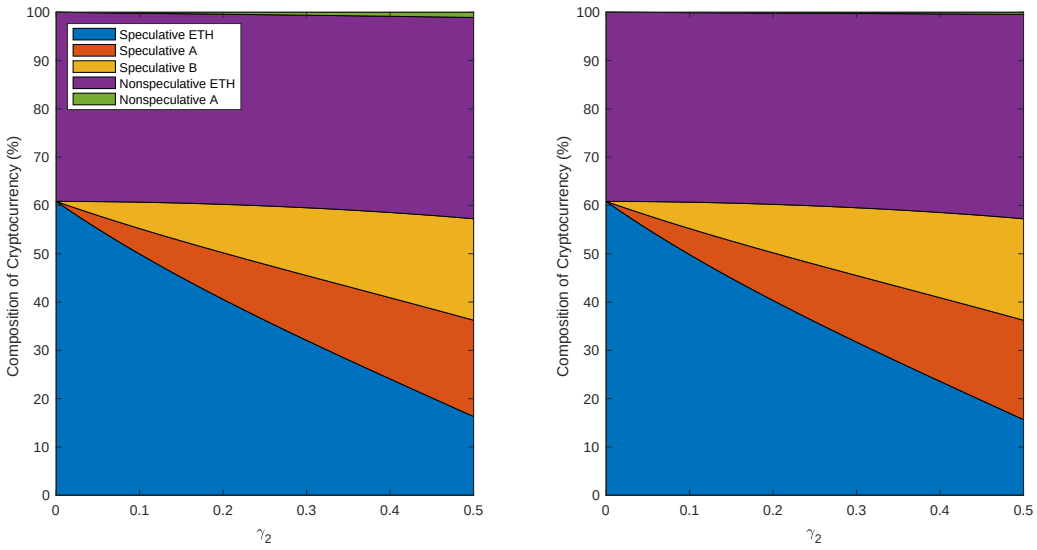

Figure 8 The impact of speculative demand in Class B on the composition of different types of demand, with $\gamma_1 = 5\%$ (left panel) and $\gamma_1 = 2\%$ (right panel). ETH is used for speculative purpose (Speculative ETH) and non-speculative purpose (Nonspeculative ETH), e.g. for payment over Ethereum network or as medium of exchange. Class A is used as a bond by speculators, and for non-speculative purpose, e.g. as a medium of exchange. Class B is only for speculative purpose only. Default parameters: $V^E = 0.2$, $P = G = 1$, $a = k = 100$, $\eta_1 = 1$, $\eta_2 = 0.5$, $E = 0.1$. γ_2 is the fraction of speculators' demand in B. $\gamma_1\gamma_2$ is the fraction of crypto-economy using A. As the fraction of speculative Class B use increases (i.e. γ_2 increases from 0 to 0.5), the fraction of speculative ETH use decreases, while the speculative use of Class B and the asset allocation use of Class A increase.

than that in supply, especially around the equilibrium price with only ETH (about 100). As a result, introducing Class A and B results in a reduction in the equilibrium price of ETH.

4. Valuation

This section is devoted to the valuation of coins described in Section 2, including Class A, B, A′ , and B′ coins. We study their fair values in terms of a stochastic representation and the corresponding partial differential equation (PDE) under the geometric Brownian motion assumption.

4.1. Class A and B coins

Denote the relative underlying value $S_t = P_t/(\beta_t P_0)$. Let W_A^t and W_B^t be the market value of Class A coins and B coins, respectively. Then the parity relation can be rewritten as $W_A^t + W_B^t = 2S_t$, which allows us to focus on the valuation of Class A coins.

Since the future cash flow of the coins depends on the cumulative time from last payment (namely, last reset or last regular payout), rather than the calendar time, in the remaining of this chapter

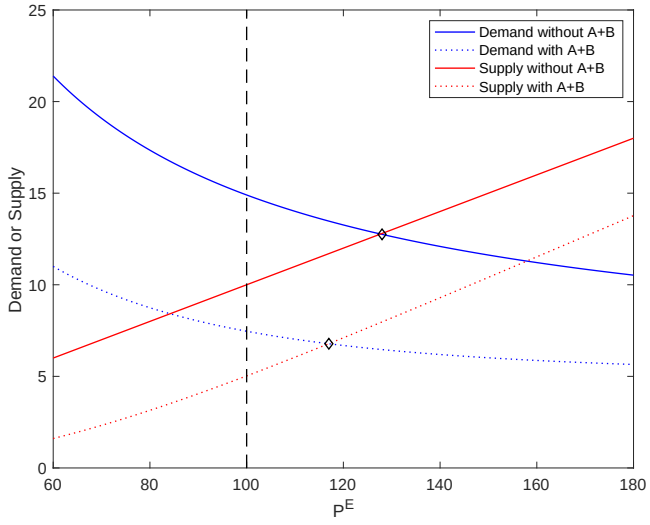

Figure 9 Supply and Demand Curve of ETH before and after introducing Stable Coins. P^E is the ETH price. After the introduction of A+B, both the demand and supply of ETH drop. For instance, at the ETH price level 100 (the vertical dashed line), the ETH demand drops from 14.9 to 7.5, and the ETH supply drops from 10.0 to 5.0. Furthermore, the equilibrium price after the introduction of A+B (the lower diamond mark) is lower than that before the introduction. Default parameters: $V^E = 0.2$, $P = G = 1$, $a = k = 100$, $\eta_1 = 1$, $\eta_2 = 0.5$, $E = 0.1$, $\gamma_1 = 0.05$, $\gamma_2 = 0.5$.

we shall relabel the last payment time as 0, so that $t \in [0,T]$ denotes the time from last payment. Denote by

$$H_d(t) = \frac{1}{2}(1+Rt) + \frac{1}{2}\mathcal{H}_d, \quad H_u(t) = \frac{1}{2}(1+Rt) + \frac{1}{2}\mathcal{H}_u$$

the downward reset barrier and the upward reset barrier (associated with S_t), respectively. Hence the downward (upward) reset is triggered when S_t hits $H_d(t)$ ($H_u(t)$). Note that the upward reset barrier H_u is time-dependent, in contrast to the dual-purpose fund in China which has a constant upward reset barrier. It is easy to see $H_d(t) \le S_t \le H_u(t)$ if S_t changes continuously. By design, S returns to 1 on every reset date, and is reduced by $\frac{1}{2}RT$ on every regular payout date.

The market value of Class A coins, $W_A^t \equiv W_A(t,S)$, is given recursively as

$$\begin{aligned} W_A(t,S) = E_t\Big[& e^{-r(T-t)}[RT + W_A(0, S_T - RT/2)] \cdot \mathbf{1}_{\{T<\tau\wedge\eta\}} + e^{-r(\tau-t)}[R\tau + W_A(0,1)] \cdot \mathbf{1}_{\{\tau\le T\wedge\eta\}} \\ & + e^{-r(\eta-t)}[R\eta + 1 - |V_B^\eta| + (V_B^\eta)^+ W_A(0,1)] \cdot \mathbf{1}_{\{\eta\le T\wedge\tau\}}\Big], \end{aligned} \tag{5}$$

where r is the risk-free rate, random times τ and η represent the first upward and downward reset date from t, respectively (i.e., $\tau = \inf\{\xi \ge t : S_\xi \ge H_u(\xi)\} \equiv \inf\{\xi \ge t : V_B^\xi \ge \mathcal{H}_u\}$ and $\eta = \inf\{\xi \ge t : S_\xi \le H_d(\xi)\} \equiv \inf\{\xi \ge t : V_B^\xi \le \mathcal{H}_d\}$), and E_t is the expectation computed under a risk-adjusted

measure and under the initial condition $S_t = S$. For example, one can assume that P follows a geometric Brownian motion under the risk-adjusted measure:

$$dP_t = rP_t dt + \sigma P_t d\mathcal{B}_t, \tag{6}$$

where $\mathcal{B}_t$ is a one-dimensional standard Brownian motion.

The value of Class A coin can be determined as above in a recursive manner, since the holders still get (certain shares of) Class A coin as well as coupons after reset or regular payout. On the right hand side of (5), the first term indicates that on the regular payout date T, holders get coupon payment RT and a new Class A coin for which the time from last payment returns to 0 and S is reduced by $RT/2$; the second term indicates that upon upward reset time τ, holders get coupon payment $R\tau$ and a new Class A coin for which the time from last payment returns to 0 and S becomes 1; and the third term indicates that upon downward reset time η, holders receive coupon payment $R\eta$, withdrawal value $1-|V_B^\eta|$, and $(V_B^\eta)^+$ shares of new Class A coin for which the time from last reset returns to 0 and S becomes 1.

Note that a simulation-based method (e.g. Adams and Clunie (2006)) may not be efficient to achieve real-time calculation of W_A, because the cash flow of Class A coins has an infinite horizon and a weakly path-dependent nature. Therefore, in the following we propose an efficient PDE-based estimation method to compute W_A under the geometric Brownian assumption (6). Since there is no overshoot by a diffusion process, V_B always equals $\mathcal{H}_d$ on downward reset. Therefore, (5) can be simplified to

$$\begin{aligned} W_A(t,S) = E_t\Big[& e^{-r(T-t)}(RT + W_A(0, S_T - RT/2)) \cdot \mathbf{1}_{\{T<\tau\wedge\eta\}} + e^{-r(\tau-t)}(R\tau + W_A(0,1)) \cdot \mathbf{1}_{\{\tau\le T\wedge\eta\}} \\ & + e^{-r(\eta-t)}(R\eta + 1 - \mathcal{H}_d + \mathcal{H}_d W_A(0,1)) \cdot \mathbf{1}_{\{\eta\le T\wedge\tau\}}\Big]. \end{aligned} \tag{7}$$

THEOREM 3. *W_A is the unique classical solution to the following partial differential equation on $\{(t,S) : 0 \le t < T, H_d(t) < S < H_u(t)\}$ with nonlocal terminal and boundary conditions:*

$$-\frac{\partial W_A}{\partial t} = \frac{1}{2}\sigma^2 S^2 \frac{\partial^2 W_A}{\partial S^2} + rS\frac{\partial W_A}{\partial S} - rW_A, \qquad 0 \le t < T,\ H_d(t) < S < H_u(t) \tag{8}$$

$$W_A(T,S) = RT + W_A(0, S - \frac{1}{2}RT), \qquad H_d(T) < S < H_u(T) \tag{9}$$

$$W_A(t, H_u(t)) = Rt + W_A(0,1), \qquad 0 \le t \le T \tag{10}$$

$$W_A(t, H_d(t)) = Rt + 1 - \mathcal{H}_d + \mathcal{H}_d W_A(0,1), \qquad 0 \le t \le T. \tag{11}$$

By classical solution we mean $W_A \in C^{1,2}(Q) \cap C(\overline{Q}\backslash D)$, where $Q = \{(t,S) : 0 \le t < T, H_d(t) < S < H_u(t)\}$ and $D = \{T\} \times \{H_d(T), H_u(T)\}$.

Theorem 3 is a special case of Theorem 5 in Appendix E of the online supplement. Basically to show Theorem 5, one has to first rewrite the expectation in $W_A(t,S)$ in a non-recursive way (see Proposition 1), and then get the unique PDE representation.

The terminal and boundary conditions (9) – (11) are directly related with the cash flow of Class A coins. Note that these conditions depend on the solution W_A itself. Such nonlocal terminal and boundary conditions make the PDE problem significantly different from the classical Black-Scholes model, leading to challenges in both theory and computation. On the theoretical aspect, due to the nonlocal conditions, the linkage between the stochastic representation (7) and the PDE problem (8) – (11) is not straightforward, and no analytical solution is available. On the numerical aspect, the nonlocalness makes the problem nonlinear, which motivates us to propose an efficient iterative procedure to find numerical solutions.

4.2. Numerical Procedure for the Pricing Equation

We propose an iterative algorithm to obtain a numerical solution of the periodic parabolic terminal-boundary value problem (8) – (11).

Algorithm 1

1. Set the initial guess $W_A^{(0)} = 0$.
2. For $i = 1, 2, \cdots$: Given $W_A^{(i-1)}$, solve for $W_A^{(i)}$, the solution to the equation

$$\begin{aligned}
-\frac{\partial W_A}{\partial t} =& \frac{1}{2}\sigma^2 S^2 \frac{\partial^2 W_A}{\partial S^2} + rS\frac{\partial W_A}{\partial S} - rW_A && 0 \le t < T, H_d(t) < S < H_u(t) \\
W_A(1,S) =& RT + W_A^{(i-1)}(0, S - \frac{1}{2}RT) && H_d(t) < S < H_u(t) \\
W_A(t, H_u(t)) =& Rt + W_A^{(i-1)}(0,1) && 0 \le t \le T \\
W_A(t, H_d(t)) =& Rt + 1 - \mathcal{H}_d + \mathcal{H}_d W_A^{(i-1)}(0,1) && 0 \le t \le T.
\end{aligned}$$

3. If $||W_A^{(i)} - W_A^{(i-1)}|| <$ tolerance, stop and return $W_A^{(i)}$; otherwise set $i = i+1$ and go to step 2.

THEOREM 4. *The sequence $(W_A^{(k)})_{k\ge 1}$ defined in Algorithm 1 is monotonically increasing, and it converges to W_A uniformly.*

4.3. Class A′ and B′ Coins

Denote by $W_{A'}(t,S)$ and $W_{B'}(t,S)$ the market prices of Class A′ and B′ coins, respectively. Since two shares of Class A coin exchange for one A′ coin and one B′ coin, i.e., $2W_A(t,S) = W_{A'}(t,S) + W_{B'}(t,S)$, in the following we only discuss the valuation of Class A′ coin. Under the risk-neutral pricing framework, $W_{A'}(t,S)$ is given recursively as

$$\begin{aligned}
E_t\Big[& e^{-r(T-t)}(R'T + W_{A'}(0, S_T - RT/2)) \cdot \mathbf{1}_{\{T<\tau\wedge\eta\}} + e^{-r(\tau-t)}(R'\tau + W_{A'}(0,1)) \cdot \mathbf{1}_{\{\tau\le T\wedge\eta\}} \\
& + e^{-r(\eta-t)}\left(\min\{R'\eta + 1 - (V_B^\eta)^+, 2(R\eta + 1 + V_B^\eta)^+\} + (V_B^\eta)^+ W_{A'}(0,1)\right)\mathbf{1}_{\{\eta\le T\wedge\tau\}}\Big], \qquad (12)
\end{aligned}$$

where τ and η are the first upward and downward reset of Class A (or equivalently, Class A$'$ and B$'$) after t, respectively. On downward reset, if $V_B^\eta > 0$, Class A$'$ receives coupon $R'\eta$, $1 - V_B^\eta$ shares of A$'$ is liquidated, and A$'$ receives the liquidation value; if $\frac{R'\eta-1}{2} - R\eta \le V_B^\eta \le 0$, A$'$ is fully liquidated, and still receives full net asset value; otherwise, A$'$ is fully liquidated and takes a loss by receiving $2(1 + R\eta + V_B^\eta)^+$ which is smaller than its net asset value $1 + R\eta$. Recall that Class A will suffer a loss if $V_B^\eta < 0$ on downward reset, therefore Class A$'$ is safer than Class A since it can still recover its full net asset value in this case, provided $V_B^\eta \ge \frac{R'\eta-1}{2} - R\eta$; only when $V_B^\eta < \frac{R'\eta-1}{2} - R\eta$ will Class A$'$ take a loss.

Assuming that P_t follows a geometric Brownian motion, then the no overshot of P_t implies that (12) reduces to

$$E_t\Bigg[e^{-r(T-t)}(R'T + W_{A'}\ (0, S_T - RT/2)) \cdot \mathbf{1}_{\{T<\tau\wedge\eta\}} + e^{-r(\tau-t)}(R'\tau + W_{A'}(0,1)) \cdot \mathbf{1}_{\{\tau\le T\wedge\eta\}}$$
$$+ e^{-r(\eta-t)}\left(R'\eta + 1 - \mathcal{H}_d + \mathcal{H}_d W_{A'}(0,1)\right) \cdot \mathbf{1}_{\{\eta\le T\wedge\tau\}}\Bigg].$$

Similar to the linkage between (7) and (8)-(11), we can prove similarly as in Theorem 3 that $W_{A'}(t,S)$ satisfies the following PDE:

$$-\frac{\partial W_{A'}}{\partial t} = \frac{1}{2}\sigma^2 S^2 \frac{\partial^2 W_{A'}}{\partial S^2} + rS\frac{\partial W_{A'}}{\partial S} - rW_{A'}, \qquad 0 \le t < T, H_d(t) < S < H_u(t) \tag{13}$$
$$W_{A'}(T,S) = R'T + W_{A'}(0, S - \frac{1}{2}RT), \qquad H_d(T) < S < H_u(T)$$
$$W_{A'}(t, H_u(t)) = R't + W_{A'}(0,1), \qquad 0 \le t \le T$$
$$W_{A'}(t, H_d(t)) = R't + 1 - \mathcal{H}_d + \mathcal{H}_d W_{A'}(0,1), \qquad 0 \le t \le T. \tag{14}$$

The above periodic PDE can be solved using a similar algorithm as in Theorem 4.

4.4. The Design with Subsidy from Class A to B

Under the contract design in Section 2.4 where Class A subsidizes Class B on downward resets, the formulas for market value of Class A and A$'$ can be adapted to reflect the difference in the cash flow on downward resets. Specifically, using the same set of notations, the market price of Class A coins with subsidy from A to B, $\tilde{W}_A(t,S)$, can now be written recursively as

$$E_t\Bigg[e^{-r(T-t)}[RT + \tilde{W}_A(0, S_T - RT/2)] \cdot \mathbf{1}_{\{T<\tau\wedge\eta\}} + e^{-r(\tau-t)}[R\tau + \tilde{W}_A(0,1)] \cdot \mathbf{1}_{\{\tau\le T\wedge\eta\}}$$
$$+ e^{-r(\eta-t)}[(R\eta - \tilde{R}\eta + 1 - |V_B^\eta|)^+ + (V_B^\eta)^+ \tilde{W}_A(0,1)] \cdot \mathbf{1}_{\{\eta\le T\wedge\tau\}}\Bigg], \tag{15}$$

and the market price of Class A′ coins, $\tilde{W}_{A'}\ (t,S)$, can be written as

$$E_t\Bigg[e^{-r(T-t)}(R'T+\tilde{W}_{A'}\ (0,S_T-RT/2))\cdot\mathbf{1}_{\{T<\tau\wedge\eta\}}+e^{-r(\tau-t)}(R'\tau+\tilde{W}_{A'}(0,1))\cdot\mathbf{1}_{\{\tau\le T\wedge\eta\}}$$
$$+e^{-r(\eta-t)}\left(\min\{R'\eta+1-(V_B^\eta)^+,2(R\eta-\tilde{R}\eta+1+V_B^\eta)^+\}+(V_B^\eta)^+\tilde{W}_{A'}(0,1)\right)\mathbf{1}_{\{\eta\le T\wedge\tau\}}\Bigg], \quad (16)$$

Assuming that P_t follows a geometric Brownian motion, similar to the linkage between (7) and PDE (8) – (11), we can prove similarly that $W_A(t,S)$ satisfies the following PDE

$$\begin{aligned}
&-\frac{\partial\tilde{W}_A}{\partial t}=\frac{1}{2}\sigma^2S^2\frac{\partial^2\tilde{W}_A}{\partial S^2}+rS\frac{\partial\tilde{W}_A}{\partial S}-r\tilde{W}_A, && 0\le t<T,\ H_d(t)<S<H_u(t)\\
&\tilde{W}_A(T,S)=RT+\tilde{W}_A(0,S-\frac{1}{2}RT), && H_d(T)<S<H_u(T)\\
&\tilde{W}_A(t,H_u(t))=Rt+\tilde{W}_A(0,1), && 0\le t\le T\\
&\tilde{W}_A(t,H_d(t))=(R-\tilde{R})t+1-\mathcal{H}_d+\mathcal{H}_d\tilde{W}_A(0,1), && 0\le t\le T,
\end{aligned}$$

and $W^t_{A'}$ satisfies the PDE (13) – (14) (after replacing $W_{A'}$ by $\tilde{W}_{A'}$).

5. Numerical Examples

For illustration, we use ETH as the underlying cryptocurrency, during the period from August 7, 2015 (its first trading date) to August 31, 2018. We divide this sample period into two sub-periods: the August 7, 2015 to September 30, 2017 for parameter estimation, and October 1, 2017 to August 31, 2018 for out-of-sample pricing and performance evaluation.[12] We further assume that the price is monitored on a *daily* basis, and the upward and downward resets are performed according to the end-of-day prices.[13] The default model parameters are: $R=0.02\%$ (7.3% p.a.), $R'=0.0082\%$ (3% p.a.), $\mathcal{H}_u=2$, $\mathcal{H}_d=0.25$, $\tilde{R}=0.0274\%$ (10% p.a.), $r=0.0082\%$ (3% p.a.), $\sigma=0.0868$ (169% p.a.), $T=100$.

5.1. Market Values of Class A and Class B

We first compute the market values of Class A and Class B coins, based on the geometric Brownian motion assumption and on the historical prices of ETH. Figure 10 shows that, although Class A has a fixed coupon rate, and its coupon payment is periodic and protected by the resets, its value is still volatile on non-coupon dates. This should be compared to the behavior of a junk bond, whose value

[12] The dual class structure of the stable coin is independent of the choice of underlying cryptocurrency; however, the liquidity and popularity of the underlying price pair do impact the viability of the structure as market arbitrage is important to ensure the structure trades as designed. In this paper, ETH/USD is used as the underlying price pair, but other popular ERC20 tokens, such as EOS, ADA, paired with major fiat other than USD, can also be considered.

[13] In practice, the price can be updated at a higher frequency (e.g. hourly) and a reset can occur during the day once a price update triggers the reset. For example, the price can be collected on a hourly basis as the volume-weighted average of the last-five-minute median prices from four exchanges and fed into the smart contract as a fix. At the currency capacity, processing 10,000 accounts only takes about 375 seconds, which is very efficient.

is influenced by its issuer's credit risk. In contrast, the main risk of Class A is not credit risk, but the risk of a downward reset. On a downward reset, a portion of Class A coins will be liquidated, so the investor will lose the value of future coupons that would be generated from this portion. Therefore, an approaching downward reset will pull down the value of Class A. This is illustrated in Figure 10 at the end of January: as the downward reset approaches, the value of Class A also goes down, especially when the model underestimates the ETH volatility (by setting $\sigma = 0.0262$ per day (annualized 0.5)).

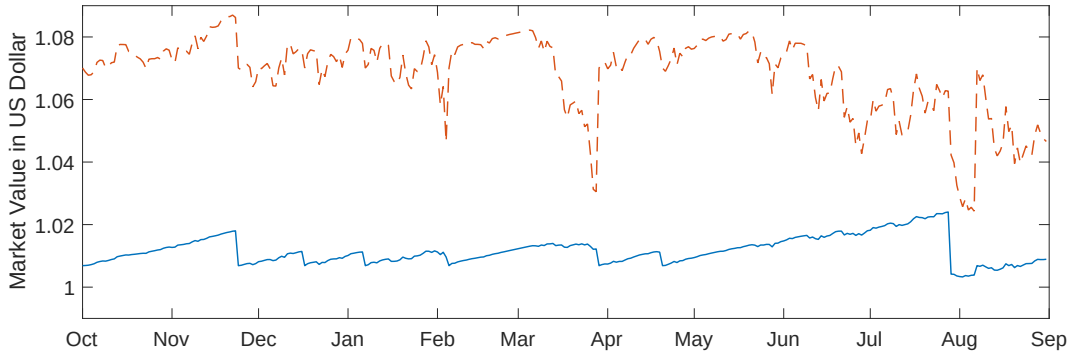

Figure 10 Simulated Class A Market Value per Share in USD. Underlying volatility parameter $\sigma = 0.0868$ for the blue solid curve, and $\sigma = 0.0262$ for the red dashed curve. Other parameters: $R = 0.02\%, \mathcal{H}_d = 0.25$, $\mathcal{H}_u = 2$, $T = 100$, $r = 0.0082\%$ per day (3% per year). Volatility of Class A market value: 2.69% under $\sigma = 0.0868$, and 9.83% under $\sigma = 0.0262$. Upward reset takes place on November 24, 2017, December 17, 2017, January 7, 2018, and April 20, 2018. Downward reset takes place on February 5, 2018, March 29, 2018 and August 07, 2018. Regular payout takes place on July 28, 2018.

Figure 11 shows the simulated paths from Class B coins. Note that Class B has upward resets (on November 24, 2017, December 17, 2017, January 7, 2018, and April 20, 2018) with dividend payments \$1.0846, \$1.0467, \$1.1106 and \$1.2108, downward resets (on February 5, 2018, March 29, 2018 and August 07, 2018), and a regular payout (on July 28, 2018).

5.2. Market Value of Class A′ and B′

We can see from Figure 12 that the market value of Class A′ coins is very stable during our sample period, with a value close to 1, except for seven downward jumps. These downward jumps correspond to the coupon payment of Class A′ on the reset dates of Class A. Therefore, from the Class A′ holders point of view, these downward jumps do not necessarily result in a loss due to the delivery of the coupon payments.

By assuming that all coupons are reinvested back into Class A′ coins, the total return of holding Class A′ coins has an annualized volatility of 0.0025% (0.0712% by assuming that coupons are held without any reinvestment), which is much smaller than that of the total return of holding Class A coins (0.76%), and is even lower than 0.0752% of the S&P U.S. Treasury Bill 0–3 Month Index.

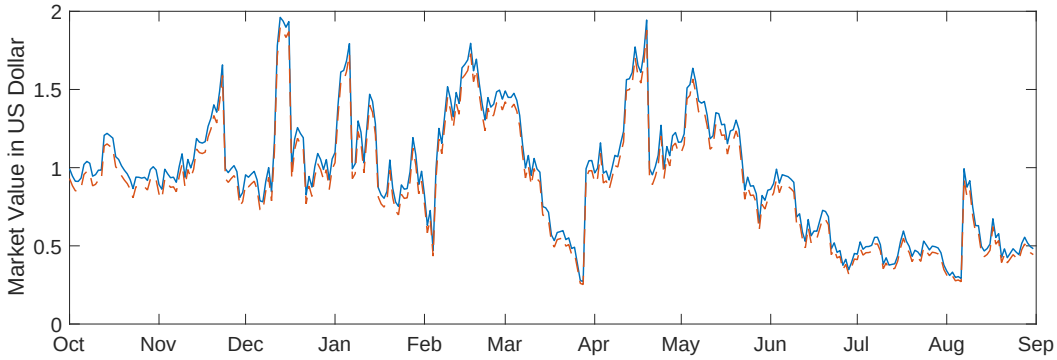

Figure 11 **Class B Market Value per Share in USD. Underlying volatility parameter $\sigma = 0.0868$ for the blue solid curve, $\sigma = 0.0262$ for the red dashed curve. Other parameters: $R = 0.02\%$, $\mathcal{H}_d = 0.25$, $\mathcal{H}_u = 2$, $T = 100$, $r = 0.0082\%$ per day (3% per year). Volatility of Class B market value: 327.22% under $\sigma = 0.0868$ and 334.52% under $\sigma = 0.0262$. Upward reset takes place on November 24, 2017, December 17, 2017, January 7, 2018, and April 20, 2018. Downward reset takes place on February 5, 2018, March 29, 2018 and August 07, 2018. Regular payout takes place on July 28, 2018.**

Even by ignoring the coupon payments and only considering the nominal price, Class A′ still has an annualized return volatility of 1.14%, which is still lower than 4.05% of the the S&P U.S. AAA Investment Grade Corporate Bond Index (from October 1, 2017 to August 31, 2018).

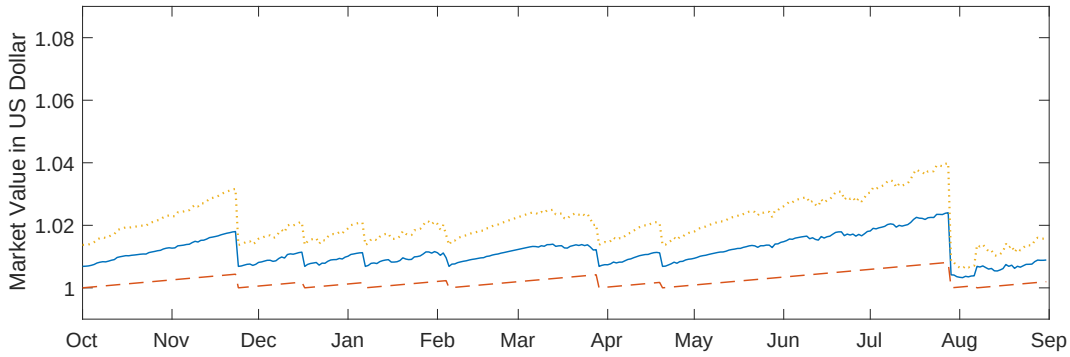

Figure 12 **Market Value of Class A′ (red) and B′ (yellow) per Share in USD, compared with Class A (blue). Value calculated under the geometric Brownian motion assumption. Annualized market value volatility of Class A′ and B′ are 1.14% and 4.30%, respectively. Parameters: $R = 0.02\%$ per day, $\mathcal{H}_d = 0.25$, $\mathcal{H}_u = 2$, $R' = 0.0082\%$ (3% per year), $T = 100$, $\sigma = 0.0868\%$, $r = 0.0082\%$ per day. Upward reset takes place on November 24, 2017, December 17, 2017, January 7, 2018, and April 20, 2018. Downward reset takes place on February 5, 2018, March 29, 2018 and August 07, 2018. Regular payout takes place on July 28, 2018.**

5.3. Market Values under Design with Subsidy from Class A to B

Under the design with a subsidy from Class A to B, Figure 13 shows that the volatilities of nominal price of Class A and A′ do not change significantly, being 2.65% and 1.14% (compared to 2.69% and

1.14%), respectively. Furthermore, the volatility of the total return of holding Class A′ also remains the same (0.0025%). The total return volatility of Class A becomes higher at 1.34% (as compared to 0.75% without the subsidy), which can be partly attributed to the sharp increase as a regular payout draws near (see, for instance, the increase around the end of November 2017 and July 2018).

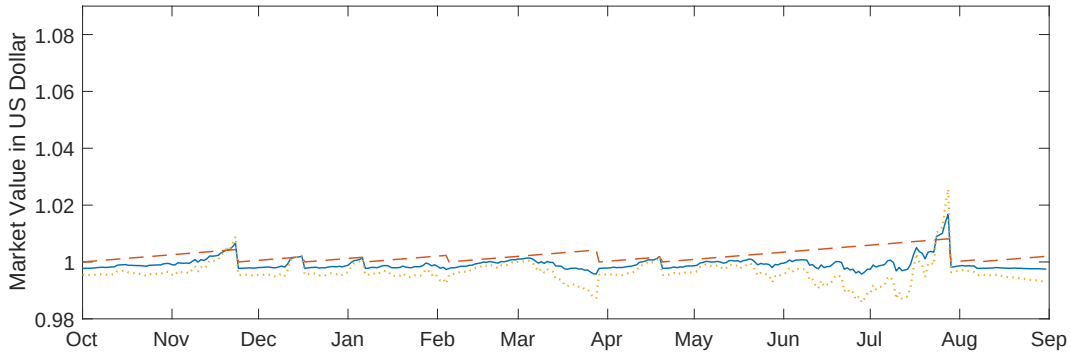

Figure 13 Market Value of Class A′ (red) and B′ (yellow) per Share in USD, compared with Class A (blue), under the design with subsidy from A to B. Value calculated under the geometric Brownian motion assumption. Annualized market value volatility of Class A′, B′ and A are 1.14%, 4.51% and 2.65%, respectively. Parameters: $R = 0.02\%$ **per day,** $\mathcal{H}_d = 0.25$, $\mathcal{H}_u = 2$, $R' = 0.0082\%$ **(**3% **per year),** $\tilde{R} = 0.0274\%$ **(**10% **per year),** $T = 100$, $\sigma = 0.0868\%$, $r = 0.0082\%$ **per day. Upward reset takes place on November 24, 2017, December 17, 2017, January 7, 2018, and April 20, 2018. Downward reset takes place on February 5, 2018, March 29, 2018 and August 07, 2018. Regular payout takes place on July 28, 2018.**

6. Jump Risk

In this section, we extend the above geometric Brownian motion based model for the ETH price to a jump diffusion model, to illustrate the performance of the stable coins in presence of the event risk (c.f. Liu et al. (2003)). To this end, we assume that the ETH price has the following risk-adjusted dynamics[14]

$$dP_t/P_{t-} = rdt + \sigma d\mathcal{B}_t + d\sum_{\tau_j \le t}(U_j - 1),$$

where $\{U_j\}$, being nonnegative and i.i.d., are the jump size following distribution ν, and $(\tau_j)_{j\ge 1}$ is the sequence of jump times of a Poisson process with intensity λ. We assume that the jump distribution ν is of double-exponential type, that is

$$\nu(dz) = \left(p\eta_1 e^{-\eta_1 z}\mathbf{1}_{\{z\ge 0\}} + (1-p)\eta_2 e^{\eta_2 z}\mathbf{1}_{\{z<0\}}\right)dz.$$

[14] If one assumes that complete hedging is possible, then the risk adjust measure is exactly the risk-neutral measure. However, even if one does not use the complete hedging argument, the standard option pricing theory using the rational expectations still gives the same dynamics, except that the risk free rate r is now endogenously determined in equilibrium by other factors, e.g. an outside endowment process; see, e.g. Kou (2002).

This distribution features both a high peak and heavy tails. We estimate the model parameters p, η_1, η_2 by following the two-step procedure in Dang and Forsyth (2016). In the first step, we choose a threshold value k, and jointly identify jumps and estimate volatility, where jumps are defined as the returns with absolute value greater than k times the volatility. In the second step, we fit the jump part and the remaining non-jump part of the returns to the double exponential distribution and normal distribution, respectively. By choosing three different values $k = 2.5, 3, 3.5$, the estimated parameters as well as the resulted out-of-sample annualized volatility are given in Table 4.

The result shows that, even after factoring in the event-based jump risk, Class A′ coins still have a very low volatility. Indeed, even by taking $k = 3.5$, Class A′ under the design without subsidy has a total return volatility 0.0696%, which is still lower than 0.0752% of the S&P U.S. Treasury Bill Index. For the design with subsidy, the volatilities become slightly larger in most cases, due to the higher probability of losses on a downward reset triggered by a large downward jump. However, even by taking $k = 3.5$, Class A′ still has a very low total return volatility 0.1161%.

Table 4 Parameter Estimation for Jump Diffusion, and Out-of-Sample Annualized Volatility

Panel A: Parameter Estimation

k	p	η_1	η_2	λ	σ
2.5	0.6555	6.0134	4.9574	0.1516	0.0435
3.0	0.5333	3.8657	3.3078	0.0382	0.0639
3.5	0.4118	3.1776	2.9385	0.0217	0.0691

Panel B: Contract Design without Subsidy

	Nominal Value		Total Return	
k	A	A′	A	A′
2.5	4.93%	1.14%	6.22%	0.0025%
3.0	10.76%	1.14%	12.73%	0.0026%
3.5	15.67%	1.14%	13.91%	0.0696%
No Jump	2.69%	1.14%	0.75%	0.0025%

Panel C: Contract Design with Subsidy

	Nominal Value		Total Return	
k	A	A′	A	A′
2.5	5.18%	1.14%	6.55%	0.0025%
3.0	10.73%	1.14%	13.12%	0.0026%
3.5	15.07%	1.13%	14.04%	0.1161%
No Jump	2.65%	1.14%	1.34%	0.0025%

In this table, Panel A presents the parameter estimation for the double-exponential jump diffusion model under $k = 2.5, 3, 3.5$; Panel B (resp. Panel C) shows the annualized volatility of the nominal value and total return portfolio of Class A and A′ without (resp. with) subsidy, under the jump diffusion model and under the geometric Brownian motion model. The parameter estimation is based on the time period August 7, 2015 – September 30, 2017, and the volatility is calculated based on the simulated price of Class A and A′ during the time period October 1, 2017 – August 31, 2018.

7. A Check of Robustness: Alternative Starting Date of Numerical Results

Our previous numerical results assume that the stable coin is created on October 1, 2017. One may ask whether the results change by choosing a different creation date. In particular, what happens if the stable coin is created at a time at which the ETH price is relatively high, such that *the price stays lower than this price for a long period of time*?

To this end, we perform an alternative test assuming a creation date of February 1, 2018. As shown in Figure 1, the ETH price at this date is \$1026.19, and this price level has never been recovered from February 2, 2018 to August 31, 2018. The resulting volatility of the nominal price of Class A′, as reported in Table 5, is 1.20%, very close to 1.14% observed under the starting date of October 1, 2017. By considering the portfolio value from holding Class A′ coin and reinvesting all dividends, the volatility is 0.0023%, also close to 0.0025%.

To understand the robustness with respect to a starting date, note that the value of A′ shares depends directly on the relative underlying value $S_t = P_t/(\beta_t P_0)$. By the contract design, the relative value equals 1 at the creation date, and jumps back to 1 at every subsequent upward or downward resets. Since the upward and downward resets occur fairly frequently due to the volatile nature of ETH price, the difference between two S paths with different starting date will be eventually small, even if the ETH price at the starting date is significantly different. In particular, if these two paths share some upward or downward reset date, the relative values from both paths will remain the same after this reset.

This is illustrated in Figure 14. Although the difference between two values is relatively large in February 2018, it soon reduces to a much lower level after the downward reset at March 14, 2018. Furthermore, after the common downward reset on March 29, 2018, these two values remain the same.

8. Conclusion

Stable coins, which are cryptocurrencies pegged to other stable financial assets, are desirable for blockchain networks to be used as public accounting ledgers for payment transactions and as crypto money market accounts for asset allocation involving cryptocurrencies, whereby being often called the "Holy Grail of cryptocurrency". However, existing cryptocurrencies, such as Bitcoins, are too volatile for these purposes. By using the option pricing theory, this paper designs, for the first time to our best knowledge, several dual-class structures for cryptocurrencies that offer entitlements to fixed income cypto assets (Class A tokens), stable coins (Class A′ coins) pegged to a traditional currency, or leveraged investment opportunities (Class B and Class B′ coins). To understand the impact of the proposed coins on the speculative and non-speculative demands of cryptocurrencies, we study

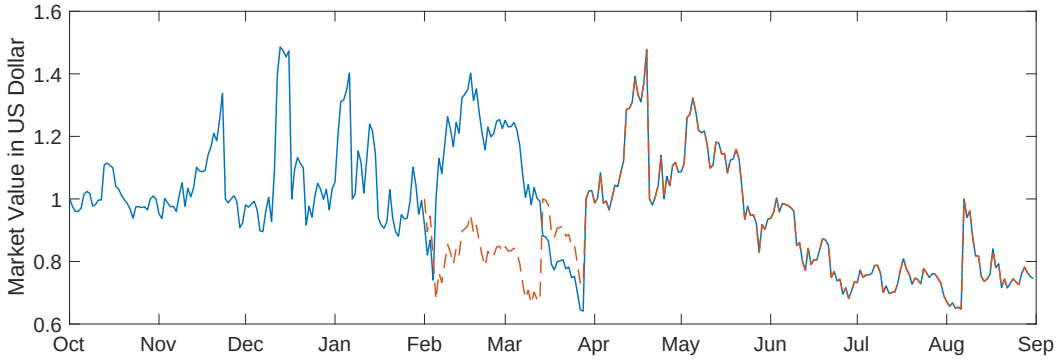

Figure 14 **Relative Value S assuming creation date October 1, 2017 (blue) and February 1, 2018 (red). For the red curve, upward reset takes place on April 19, 2018. Downward reset takes place on March 14, 2018, March 29, 2018 and August 6, 2018. Regular payout takes place on July 28, 2018. For the blue curve, upward reset takes place on November 24, 2017, December 17, 2017, January 7, 2018, and 19 Apr 2018. Downward reset takes place on February 5, 2018, March 29, 2018 and August 6, 2018. Regular payout takes place on July 28, 2018.**

Table 5 **Parameter Estimation for Jump Diffusion, and Out-of-Sample Annualized Volatility, Starting from February 1, 2018**

Panel A: Parameter Estimation

k	p	η_1	η_2	λ	σ
2.5	0.6562	6.0472	5.0246	0.1410	0.0427
3.0	0.5000	4.0972	3.7914	0.0463	0.0597
3.5	0.4737	3.3499	2.9385	0.0209	0.0670

Panel B: Contract Design without Subsidy

	Nominal Value		Total Return	
k	A	A′	A	A′
2.5	6.98%	1.20%	8.69%	0.0021%
3.0	10.23%	1.20%	14.43%	0.0022%
3.5	16.91%	1.19%	17.75%	0.0441%
No Jump	2.89%	1.20%	1.01%	0.0023%

Panel C: Contract Design with Subsidy

	Nominal Value		Total Return	
k	A	A′	A	A′
2.5	7.43%	1.20%	9.05%	0.0021%
3.0	10.88%	1.20%	14.99%	0.0022%
3.5	16.78%	1.18%	18.14%	0.0771%
No Jump	2.99%	1.20%	1.57%	0.0023%

In this table, Panel A presents the parameter estimation for the double-exponential jump diffusion model under $k = 2.5, 3, 3.5$ under the simulation starting date Feb 1, 2018; Panel B (resp. Panel C) shows the annualized volatility of the nominal value and total return portfolio of Class A and A′ without (resp. with) subsidy, under the jump diffusion model and under the geometric Brownian motion model. The parameter estimation is based on the time period August 7, 2015 – September 30, 2017, and the volatility is calculated based on the simulated price of Class A and A′ during the time period October 1, 2017 – August 31, 2018.

equilibrium with and without the stable coins. We show that the proposed stable coins have very low volatility; indeed, Class A′ coin essentially is pegged to U.S. dollar. Our investigation of the values

of stable coins in presence of jump risk and black-swan type events demonstrates the robustness of the design.

References

Adams, Andrew T., James B. Clunie. 2006. Risk assessment techniques for split capital investment trusts. *Annals of Actuarial Science* **1** 7–36.

Al-Naji, Nader. 2018. Basecoin: A price-stable cryptocurrency with an algorithmic central bank. `http://www.getbasecoin.com/basecoin_whitepaper_0_99.pdf`.

Barro, Robert J. 1979. Money and the price level under the gold standard. *The Economic Journal* **89**(353) 13–33.

Bech, Morten L., Rodney Garratt. 2017. Central bank cryptocurrencies. `https://papers.ssrn.com/abstract=3041906`.

Catalini, Christian, Joshua S. Gans. 2016. Some simple economics of the blockchain. Working Paper.

Chen, Cathy Y., Wolfgang K. Härdle, Ai Jun Hou, Weining Wang. 2018. Pricing cryptocurrency options: The case of crix and bitcoin. Working Paper.

Chen, Shi, Cathy Y. Chen, Wolfgang K. Härdle, Teik Ming Lee, Bobby Ong. 2016. A first econometric analysis of the crix family. Working Paper.

Ciaian, Pavel, Miroslava Rajcaniova, d'Artis Kancs. 2016. The economics of BitCoin price formation. *Applied Economics* **48**(19) 1799–1815.

Dai, Min, Steven Kou, Chen Yang. 2017. A stochastic representation for nonlocal parabolic PDEs with applications. Working Paper.

Dai, Min, Steven Kou, Chen Yang, Zhenfei Ye. 2018. The overpricing of leveraged products: A case study of dual-purpose funds in china. Working Paper.

Dang, Duy-Minh, Peter A. Forsyth. 2016. Better than pre-commitment mean-variance portfolio allocation strategies: A semi-self-financing Hamilton–Jacobi–Bellman equation approach. *European Journal of Operational Research* **250**(3) 827–841.

Grinberg, Reuben. 2011. Bitcoin: An innovative alternative digital currency. `https://papers.ssrn.com/abstract=1817857`.

Grunspan, Cyril, Ricardo Perez-Marco. 2018. Double spend races. Working Paper.

Harvey, Campbell R. 2016. Cryptofinance. `https://papers.ssrn.com/abstract=2438299`.

Ingersoll, Jonathan E. 1976. A theoretical and empirical investigation of the dual purpose funds: An application of contingent-claims analysis. *Journal of Financial Economics* **3** 83–123.

Jarrow, Robert A., M.A.U.R.E.E.N. O'Hara. 1989. Primes and scores: An essay on market imperfections. *The Journal of Finance* **44** 1263–1287.

Khapko, Mariana, Marius Zoican. 2018. Smart settlement. https://papers.ssrn.com/abstract=2881331.

Kou, Steven G. 2002. A jump diffusion model for option pricing. *Management Science* **48**(8) 1086–1101.

Liu, Jun, Francis A. Longstaff, Jun Pan. 2003. Dynamic Asset Allocation with Event Risk. *The Journal of Finance* **58**(1) 231–259.

MakerTeam. 2017. The Dai stablecoin system. https://makerdao.com.

Nakamoto, Satoshi. 2008. Bitcoin: A peer-to-peer electronic cash system. https://bitcoin.org/bitcoin.pdf.

Rogoff, Kenneth. 2015. Costs and benefits to phasing out paper currency. *NBER Macroeconomics Annual* **29**(1) 445–456.

Tether. 2016. Tether: Fiat currencies on the Bitcoin blockchain. https://tether.to/wp-content/uploads/2016/06/TetherWhitePaper.pdf.

The Libra Association. 2019. Libra: White paper. https://libra.org/en-US/white-paper/.

Online Supplement

Designing Stable Coins

A. Product Design with General Split Ratio

In Section 2, we have described a specific product design where Class A is stable relative to USD as target fiat currency and Class B has initial leverage as 2 ($\alpha = 1$). In addition, transaction cost in creation and redemption is omitted. In this section, a general case is discussed.

Dual-class coins can be created by depositing underlying cryptocurrency to the Custodian contract. Upon receiving underlying cryptocurrency of amount M_C, the Custodian contract will return to the sender certain amount of Class A and Class B coins. Such amount C_A and C_B can be calculated by:

$$C_B = \frac{M_C P_0 \beta_t (1-c)}{1+\alpha}, \quad C_A = \alpha C_B, \tag{17}$$

where c is the processing fee of the smart contract, α is a positive number to determine the ratio of A and B, and P_0 is the recorded price of underlying cryptocurrency in target fiat currency at last reset event, and β_t is the conversion factor set as 1 at inception and its behaviour is detailed later in Section A.1 to A.2.

Holders of Class A and Class B coins can withdraw deposited underlying cryptocurrency at any time by performing a redemption. To do this, the user will send αC amount of Class A coins and C amount of Class B coins to the Custodian contract. The contract will deduct Class A and Class B coins, and return to the sender M_C underlying cryptocurrency, where M_C can be calculated by:

$$M_C = \frac{C(1-c)(1+\alpha)}{\beta_t P_0}. \tag{18}$$

The net value of coins are calculated based on the coupon rate, the elapsed time from last reset event, and the latest underlying cryptocurrency price in target fiat currency fed to the system. In particular:

$$V_A^t = 1 + R \cdot v_t, \quad V_B^t = (1+\alpha) \cdot \frac{P_t}{\beta_t P_0} - \alpha \cdot V_A^t, \tag{19}$$

where R is the daily coupon rate, v_t is the number of days from last reset event, and P_t is the current price of underlying cryptocurrency in target fiat currency. Note that at all time $Q_A^t = \alpha Q_B^t$, where Q_A^t and Q_B^t are the total amount of Class A and Class B coins. The implied leverage ratio is

$$L_B^t = \frac{P_t}{\beta_t P_0} \cdot \frac{1+\alpha}{V_B^t}$$

Note that at inception or after contingent resets, above simply reduces to $L_B^0 = 1 + \alpha$.

A.1. Regular Payout

A regular payout is triggered when $v_{t-} = T$. Upon regular payout:

1. Total amount of both classes coin remain unchanged, $Q_A^{t+} = Q_A^{t-}$ and $Q_B^{t+} = Q_B^{t-}$
2. Net asset value of Class A reset to 1 USD
3. Class A holder will receive certain amount of underlying cryptocurrency from the Custodian contract. Such amount for each Class A coin is $U_A = \frac{V_A^t - 1}{P_t}$
4. Conversion factor $\beta_{t+} = \beta_{t-} \cdot \frac{(1+\alpha)P_t}{(1+\alpha)P_t - \alpha\beta_{t-}P_0\left(V_A^t - 1\right)}$

Total value in the system is unchanged after reset:

$$\begin{aligned} & U_A \cdot P_t \cdot Q_A^{t-} + Q_A^{t+} \cdot V_A^{t+} + Q_B^{t+} \cdot V_B^{t+} \\ =& \left(V_A^{t-} - 1\right) \cdot Q_A^{t-} + Q_A^{t-} \cdot 1 + V_B^{t-} \cdot Q_B^{t-} \\ =& V_A^{t-} \cdot Q_A^{t-} + V_B^{t-} \cdot Q_B^{t-} \ . \end{aligned}$$

A.2. Contingent Upward Reset

An upward reset is triggered when $V_B^t \geqslant \mathcal{H}_u$. Upon upward reset:

1. Total amount of both classes coins remain unchanged, $Q_A^{t+} = Q_A^{t-}$ and $Q_B^{t+} = Q_B^{t-}$.
2. Net asset value of both classes reset to 1 target fiat currency.
3. Both classes' holders will receive certain amount of underlying cryptocurrency from the Custodian contract. Such amount for each Class A coin is $U_A = \frac{V_A^t - 1}{P_t}$ and for each Class B coin is $U_B = \frac{V_B^t - 1}{P_t}$.
4. Conversion factor β_{t+} is reset to P_t/P_0.

Total value in the system is unchanged after reset:

$$\begin{aligned} & U_A \cdot P_t \cdot Q_A^t + U_B \cdot P_t \cdot Q_B^t + Q_A^{t+} \cdot V_A^{t+} + Q_B^{t+} \cdot V_B^{t+} \\ =& (V_A^t - 1) \cdot Q_A^t + (V_B^t - 1) \cdot Q_B^t + Q_A^t \cdot 1 + Q_B^t \cdot 1 \\ =& V_A^t \cdot Q_A^t + V_B^t \cdot Q_B^t \ . \end{aligned}$$

A.3. Contingent Downward Reset

A downward reset is triggered when $V_B^t \leqslant \mathcal{H}_d$. Upon downward reset:

1. Total amount of Class B coins is reduced to $Q_B^{t+} = Q_B^{t-} \cdot (V_B^t)^+$.
2. Total amount of Class A coins is reduced to $Q_A^{t+} = Q_B^{t+} \cdot \alpha$.
3. Net Value of both classes reset to 1 target fiat currency.
4. Class A holders will receive certain amount of underlying cryptocurrency from the Custodian contract. Such amount of each Class A coin is: $D_A = \frac{V_A^t - V_B^t}{P_t}$ if $V_B^t \geq 0$, and $D_A = \frac{V_A^t + V_B^t/\alpha}{P_t}$ if $V_B^t < 0$
5. Conversion factor β_{t+} is reset to P_t/P_0.

Total value in the system is unchanged after reset:

$$\begin{aligned}
&D_A \cdot P_t \cdot Q_A^{t-} + Q_A^{t+} \cdot V_A^{t+} + Q_B^{t+} \cdot V_B^{t+} \\
=&\left[(V_A^t - V_B^t) \cdot \mathbf{1}_{V_B^t \geq 0} + (V_A^t + V_B^t/\alpha) \cdot \mathbf{1}_{V_B^t < 0}\right] \cdot Q_A^{t-} + Q_B^{t+} \cdot \alpha \cdot 1 + Q_B^{t+} \cdot 1 \\
=&V_A^t \cdot Q_A^{t-} - (V_B^t)^+ \cdot Q_B^{t-} \cdot \alpha - (V_B^t)^- \cdot Q_B^{t-} + Q_B^{t-} \cdot (V_B^t)^+ \cdot \alpha + Q_B^{t-} \cdot (V_B^t)^+ \\
=&V_A^t \cdot Q_A^{t-} + V_B^t \cdot Q_B^{t-} \ .
\end{aligned}$$

Note above used the fact $Q_A^{t-} = Q_B^{t-} \cdot \alpha$.

In the absence of arbitrage, the following price parity shall hold

$$\alpha \cdot W_A^t + W_B^t = \alpha \cdot V_A^t + V_B^t \ ,$$

where W_A^t is the current price of Class A in target fiat currency, and W_B^t is the current price of Class B in target fiat currency.

B. Pricing Equations for the Jump Diffusion Models

Following Merton (1976), the pricing PDE of Class A coins, W_A, is given as

$$\begin{aligned}
-\frac{\partial W_A}{\partial t} &= \frac{1}{2}\sigma^2 S^2 \frac{\partial^2 W}{\partial S^2} + (r - \lambda(EU - 1))S\frac{\partial W}{\partial S} - rW_A \\
&\quad + \lambda \int_{\mathbb{R}^+} W_A(t, Sz)\nu(dz) - \lambda W_A(t, S) \\
W_A(T, S) &= RT + W_A(0, S - \frac{1}{2}RT) && H_d(T) < S < H_u(T) \\
W_A(t, S) &= Rt + W_A(0, 1), && 0 \leq t \leq T,\ S \geq H_u(t) \\
W_A(t, S) &= Rt + 1 - |g(t, S)| + (g(t, S))^+ W_A(0, 1), && 0 \leq t \leq T,\ 0 < S \leq H_d(t),
\end{aligned} \tag{20}$$

where $g(t, S) = 2S - (1 + Rt)$ is the net asset value of Class B coins. Similarly, the pricing PDE of Class A′ coins, $W_{A'}$, is given as

$$\begin{aligned}
-\frac{\partial W_{A'}}{\partial t} &= \frac{1}{2}\sigma^2 S^2 \frac{\partial^2 W_{A'}}{\partial S^2} + (r - \lambda(EU - 1))S\frac{\partial W_{A'}}{\partial S} - rW_{A'} \\
&\quad + \lambda \int_{\mathbb{R}^+} W_{A'}(t, Sz)\nu(dz) - \lambda W_{A'}(t, S) \\
W_{A'}(T, S) &= R'T + W_{A'}(0, S) && H_d(T) < S < H_u(T) \\
W_{A'}(t, S) &= R't + W_{A'}(0, S) && 0 \leq t \leq T, S \geq H_u(t) \\
W_{A'}(t, S) &= \min\{R't + 1 - (g(t, S))^+, 2(Rt + 1 + g(t, S))^+\} && \\
&\quad + (g(t, S))^+ W_{A'}(0, 1) && 0 \leq t \leq T, 0 < S \leq H_d(t)
\end{aligned} \tag{21}$$

The interpretation of the terminal and boundary conditions of W_A and W_A' is similar to that of (5) and (12), respectively.

The pricing PDEs of Class A and A′ coins with subsidy from A to B are the same as the above two PDEs (replacing W_A and $W_{A'}$ by $\tilde{W}_A$ and $\tilde{W}_{A'}$, respectively), expect that the lower bound conditions (20) and (21) need to be changed to

$$\tilde{W}_A(t,S) = (Rt - \tilde{R}t + 1 - |g(t,S)|)^+ + (g(t,S))^+ W_A(0,1), \qquad 0 \le t \le T,\ 0 < S \le H_d(t),$$

and

$$\begin{aligned} W_{A'}(t,S) = \min\{&R't + 1 - (g(t,S))^+, 2(Rt - \tilde{R}t + 1 + g(t,S))^+\} \qquad 0 \le t \le T, 0 < S \le H_d(t) \\ &+ (g(t,S))^+ W_{A'}(0,1), \end{aligned}$$

respectively.

C. Proof of Theorem 1

Denote

$$\varphi(P^E) = P^E E - f(P^E, a) - \frac{PG}{V^E}.$$

Note that φ is increasing since $f(P^E, a)$ is decreasing in P^E. Furthermore, $\varphi(0) = -f(0,a) - \frac{PG}{V^E} < 0$ and $\lim_{P^E \to +\infty} \varphi'(P^E) = E > 0$. Therefore, there exists a unique root $P^{E,*} > 0$ of φ.

The monotonicity follows from differentiating on $\varphi(P^E) = 0$. For illustration, we only show the monotonicity in a. Differentiating with respect to a,

$$\frac{\partial P^E}{\partial a} = \left(E - \frac{\partial f}{\partial P^E}\right)^{-1} \cdot \frac{\partial f}{\partial a}(P^{E,*}, a),$$

and the RHS is positive since $\frac{\partial f}{\partial a} > 0$ and $-\frac{\partial f}{\partial P^E} > 0$ according to Assumption 1. The remaining monotonicity claims can be derived similarly. Q.E.D.

D. Proof of Theorem 2

Denote $\varphi(P^E)$ as the difference between LHS and RHS of (4). Thanks to Assumption 1, $f(P^E, a)$ and $\frac{f(P^E,a)}{P^E}$ are both decreasing in P^E. Since g is increasing thanks to Assumption 3, $g\left(\frac{\gamma_2 f(P^E,a)}{0.5P^E}\right)$ is decreasing in P^E. Therefore, $\varphi(P^E)$ is decreasing in P^E. Next, as $P^E \to 0+$, $\varphi(P^E) \to (1-\gamma_2)\lim_{P^E \to 0+} f(P^E, a) + \frac{PG}{V^E} > 0$. As $P^E \to +\infty$, $g\left(\frac{\gamma_2 f(P^E,a)}{0.5P^E}\right) \to 0$, therefore $\varphi(P^E) \to -\infty$. Also, φ is continuous. Therefore, there exists a unique root to $\varphi = 0$.

To see that $P^{E,*}$ is increasing in a, dividing both sides of (4) by $P^{E,*}$ leads to

$$(1-\gamma_2)\hat{f}(P^{E,*}, a) + \frac{PG}{V^E P^{E,*}} - E + 0.5Eg\left(\frac{\gamma_2}{0.5}\hat{f}(P^{E,*}, a)\right) = 0,$$

where $\hat{f}(P^E, a) := \frac{f(P^E,a)}{P^E}$. Differentiating with respect to a on both sides,

$$(1-\gamma_2)\left[\frac{\partial \hat{f}}{\partial P^E}\frac{\partial P^{E,*}}{\partial a} + \frac{\partial \hat{f}}{\partial a}\right] - \frac{PG}{V^E (P^{E,*})^2}\frac{\partial P^{E,*}}{\partial a} + \gamma_2 E g' \cdot \left[\frac{\partial \hat{f}}{\partial P^E}\frac{\partial P^{E,*}}{\partial a} + \frac{\partial \hat{f}}{\partial a}\right] = 0.$$

Denote $L := 1-\gamma_2+\gamma_2 Eg'$. Since g is increasing, $L \geq 1-\gamma_2 \geq 0$. Therefore,

$$\frac{\partial P^{E,*}}{\partial a} = -L\frac{\partial \hat{f}}{\partial a} \Big/ \left(L\frac{\partial \hat{f}}{\partial P^E} - \frac{PG}{V^E (P^{E,*})^2} \right) \geq 0,$$

since $\frac{\partial \hat{f}}{\partial P^E} < 0$ and $\frac{\partial \hat{f}}{\partial a} > 0$. Q.E.D.

E. Derivation of the Pricing Equation

Using contract design under general split ratio $\alpha > 0$, similar to (5), the value of Class A coins is described by the stochastic representation

$$\begin{aligned} W_A(t,S) = E_t \Big[& e^{-r(T-t)} (RT + W_A(0, S_T - \alpha RT/(1+\alpha))) \cdot \mathbf{1}_{\{T<\tau\wedge\eta\}} \\ & + e^{-r(\tau-t)} (R\tau + W_A(0,1)) \cdot \mathbf{1}_{\{\tau \leq T\wedge\eta\}} \\ & + e^{-r(\eta-t)} (R\eta + 1 - |V_B^\eta| + (V_B^\eta)^+ W_A(0,1)) \cdot \mathbf{1}_{\{\eta \leq T\wedge\tau\}} \Big]. \end{aligned} \tag{22}$$

Note that (22) becomes (5) when $\alpha = 1$. In this section, under the geometric Brownian motion assumption, we show that (22) defines a unique bounded function W_A, which is exactly the solution to the PDE problem (8) – (11) when $\alpha = 1$. We denote v_s and Y_s as the time from last regular payout or reset and the number of A shares at time s, respectively. Starting from an initial value 1, Y is reduced by a factor of $\mathcal{H}_d$ on every downward reset dates (thanks to the geometric Brownian motion assumption), reflecting the partial payback of Class A principal. In this remaining of this section, we focus on the right limit process S_{t+}, which is still denoted as S_t for simplicity of notations. Further denote ζ_i, τ_i, and η_i as the i-th regular payout date, upward reset date, and downward reset date after t, respectively. From the construction of contract, we have

$$\begin{aligned} & dS_t = rS_t dt + \sigma S_t d\mathcal{B}_t, \\ & S_{\zeta_i} = S_{\zeta_i -} - \frac{\alpha}{\alpha+1} R v_{\zeta_i -}, \quad S_{\tau_i} = S_{\eta_i} = 1, \quad v_{\tau_i} = v_{\eta_i} = v_{\zeta_i} = 0, \end{aligned}$$

where $\mathcal{B}$ is a Brownian motion under the risk-neutral measure.

First, we derive the following proposition, which expresses the stochastic representation (22) into a non-recursive form.

PROPOSITION 1. *Equation* (22) *defines a unique solution* $W_A(t,S)$ *for* $0 \leq t \leq T$, $H_d(t) \leq S \leq H_u(t)$, *which can be written as*

$$\begin{aligned} W_A(t,S) = E_t^{(t,S,1)} \Big[& \sum_{\zeta_i \geq t} e^{-r(\zeta_i - t)} Y_{\zeta_i -} RT + \sum_{\tau_i \geq t} e^{-r(\tau_i - t)} Y_{\tau_i -} R v_{\tau_i -} \\ & + \sum_{\eta_i \geq t} e^{-r(\eta_i - t)} Y_{\eta_i -} (R v_{\eta_i -} + 1 - \mathcal{H}_d) \Big], \end{aligned} \tag{23}$$

where $E_t^{(u,s,y)}$ *is the* $\mathbb{Q}$*-expectation computed under the initial condition* $v_{t-}=u$*,* $S_{t-}=s$*, and* $Y_{t-}=y$*.*[15]

Proof of Proposition 1. Without loss of generality we prove the case $T=1$. We prove this theorem in three steps.

Step 1: To see that W_A given by (23) satisfies (22), note that (23) implies

$$\begin{aligned}
W_A(t,S) = E_t^{t,S,1}\Bigg[& \sum_{t\le\zeta_i<\tau_1\wedge\eta_1} e^{-r(\zeta_i-t)}Y_{\zeta_i-}R + e^{-r(\tau_1-t)}Y_{\tau_1-}Rv_{\tau_1-}\cdot\mathbf{1}_{\{\tau_1<\eta_1\}} \\
& + e^{-r(\eta_1-t)}Y_{\eta_1-}(Rv_{\eta_1-}+1-\mathcal{H}_d)\cdot\mathbf{1}_{\{\eta_1<\tau_1\}} \\
& + e^{-r(\tau_1\wedge\eta_1-t)}Y_{\tau_1\wedge\eta_1}E_{\tau_1\wedge\eta_1}^{(0,1,Y_{\tau_1\wedge\eta_1})}\Bigg(\sum_{\zeta_i\ge\tau_1\wedge\eta_1} e^{-r(\zeta_i-\tau_1\wedge\eta_1)}\frac{Y_{\zeta_i-}}{Y_{\tau_1\wedge\eta_1}}R \\
& + \sum_{\tau_i>\tau_1\wedge\eta_1} e^{-r(\tau_i-\tau_1\wedge\eta_1)}\frac{Y_{\tau_i-}}{Y_{\tau_1\wedge\eta_1}}Rv_{\tau_i-} \\
& + \sum_{\eta_i>\tau_1\wedge\eta_1} e^{-r(\eta_i-\tau_1\wedge\eta_1)}\frac{Y_{\eta_i-}}{Y_{\tau_1\wedge\eta_1}}(Rv_{\eta_i-}+1-\mathcal{H}_d)\Bigg)\Bigg],
\end{aligned}$$

where $E_{\tau_1\wedge\eta_1}^{(u,s,y)}$ denotes the conditional expectation computed at time $\tau_1\wedge\eta_1$ with $(v,S,Y)_{\tau_1\wedge\eta_1}=(u,s,y)$. As a result,

$$\begin{aligned}
& E_{\tau_1\wedge\eta_1}^{(0,1,Y_{\tau_1\wedge\eta_1})}\Bigg[\sum_{\zeta_i\ge\tau_1\wedge\eta_1} e^{-r(\zeta_i-\tau_1\wedge\eta_1)}\frac{Y_{\zeta_i-}}{Y_{\tau_1\wedge\eta_1}}R + \sum_{\tau_i>\tau_1\wedge\eta_1} e^{-r(\tau_i-\tau_1\wedge\eta_1)}\frac{Y_{\tau_i-}}{Y_{\tau_1\wedge\eta_1}}Rv_{\tau_i-} \\
& \quad + \sum_{\eta_i>\tau_1\wedge\eta_1} e^{-r(\eta_i-\tau_1\wedge\eta_1)}\frac{Y_{\eta_i-}}{Y_{\tau_1\wedge\eta_1}}(Rv_{\eta_i-}+1-\mathcal{H}_d)\Bigg] \\
& = E_0^{(0,1,1)}\Bigg[\sum_{\zeta_i\ge0} e^{-r\zeta_i}Y_{\zeta_i-}R + \sum_{\tau_i\ge0} e^{-r\tau_i}Y_{\tau_i-}Rv_{\tau_i-} \\
& \quad + \sum_{\eta_i\ge0} e^{-r\eta_i}Y_{\eta_i-}(Rv_{\eta_i-}+1-\mathcal{H}_d)\Bigg] \\
& = W_A(0,1),
\end{aligned}$$

where the first equality follows from the Markov property of (v,S,Y) and the fact that time 0 cannot be an coupon payment date given $(v,S,Y)_0=(0,1,1)$. Plugging this equation into the previous equation, we get

$$W_A(t,S) = E_t^{(t,S,1)}\Bigg[\sum_{t\le\zeta_i<\tau_1\wedge\eta_1} e^{-r(\zeta_i-t)}Y_{\zeta_i-}R + e^{-r(\tau_1-t)}Y_{\tau_1-}Rv_{\tau_1-}\cdot\mathbf{1}_{\{\tau_1<\eta_1\}}$$

[15] If t and S are such that t is a regular payout or downward/upward reset date, the right hand side of (5) is viewed as the value of the time-t payment plus the expectation with the value of state variables immediately after the jump (if applicable) as time-t starting values.

$$+ e^{-r(\eta_1-t)}Y_{\eta_1-}(Rv_{\eta_1-}+1-\mathcal{H}_d)\cdot\mathbf{1}_{\{\eta_1<\tau_1\}}+e^{-r(\tau_1\wedge\eta_1-t)}Y_{\tau_1\wedge\eta_1}W_A(0,1)\Bigg]$$

$$= E_t^{(t,S,1)}\Bigg[\sum_{\zeta_i<\tau_1\wedge\eta_1} e^{-r(\zeta_i-t)}R + e^{-r(\tau_1-t)}R(\tau_1-\lfloor\tau_1\rfloor+W_A(0,1))\cdot\mathbf{1}_{\{\tau_1<\eta_1\}}$$

$$+ e^{-r(\eta_1-t)}(R(\eta_1-\lfloor\eta_1\rfloor)+1-\mathcal{H}_d+\mathcal{H}_dW_A(0,1))\cdot\mathbf{1}_{\{\eta_1<\tau_1\}}\Bigg]$$

by the definition of v, Y, and ζ. This yields (22).

Step 2: Next we show that any solution W_A satisfying (22) is a bounded function of (t,S) in $0\le t\le 1$, $H_d(t)\le S\le H_u(t)$. Indeed,

$$\begin{aligned}
W_A(t,S) &= E_t^{(t,S,1)}\Bigg[\sum_{1\le i<\tau\wedge\eta} e^{-r(i-t)}R + e^{-r(\tau-t)}\Bigg(R(\tau-\lfloor\tau\rfloor)\\
&\quad + W_A(0,1))\cdot\mathbf{1}_{\{\tau<\eta\}}\\
&\quad + e^{-r(\eta-t)}(R(\eta-\lfloor\eta\rfloor)+1-\mathcal{H}_d+\mathcal{H}_dW_A(0,1)\Bigg)\cdot\mathbf{1}_{\{\eta<\tau\}}\Bigg]\\
&\le E_t^{(t,S,1)}\Bigg[\sum_{1\le i<\tau\wedge\eta} e^{-r(i-t)}R\\
&\quad + e^{-r(\tau\wedge\eta-t)}(R+\max\{W_A(0,1),1-\mathcal{H}_d+\mathcal{H}_dW_A(0,1)\})\Bigg]\\
&\le \frac{e^{-r}R}{1-e^{-r}} + (R+\max\{W_A(0,1),1-\mathcal{H}_d+\mathcal{H}_dW_A(0,1)\}) := \overline{K}.
\end{aligned}$$

Note that the right hand side does not depend on t or S.

Step 3: To see the uniqueness, for any W_A satisfying (22), by defining the first coupon payment time $\theta_1=\tau_1\wedge\eta_1\wedge 1$, we get

$$\begin{aligned}
W_A(t,S) &= E_t^{(t,S,1)}\Bigg[e^{-r(\theta_1-t)}\Bigg((R+W_A(0,S_{\theta_1-}-\alpha R/(1+\alpha)))\cdot\mathbf{1}_{\{\theta_1<\tau_1\wedge\eta_1\}}\\
&\quad + (R(\theta_1-\lfloor\theta_1\rfloor)+W_A(0,1))\cdot\mathbf{1}_{\{\theta_1=\tau_1\}}\\
&\quad + (R(\theta_1-\lfloor\theta_1\rfloor)+1-\mathcal{H}_d+\mathcal{H}_dW_A(0,1))\cdot\mathbf{1}_{\{\theta_1=\eta_1\}}\Bigg)\Bigg]\\
&= E_t^{(t,S,1)}\Bigg[e^{-r(\theta_1-t)}\Bigg(R\cdot\mathbf{1}_{\{\theta_1=\zeta_1\}}+Rv_{\theta_1-}\cdot\mathbf{1}_{\{\theta_1=\tau_1\}}\\
&\quad + (Rv_{\theta_1-}+1-\mathcal{H}_d)\cdot\mathbf{1}_{\{\theta_1=\eta_1\}}+Y_{\theta_1}W_A(v_{\theta_1},S_{\theta_1})\Bigg)\Bigg].
\end{aligned}$$

Therefore,

$$W_A(t,S)$$

$$= E_t^{(t,S,1)}\Bigg[\sum_{\zeta_i\le\theta_1} e^{-r(\zeta_i-t)}Y_{\zeta_i-}R + \sum_{\tau_i\le\theta_1} e^{-r(\tau_i-t)}Y_{\tau_i-}Rv_{\tau_i-}$$
$$+ \sum_{\eta_i\le\theta_1} e^{-r(\eta_i-t)}Y_{\eta_i-}(Rv_{\eta_i-}+1-\mathcal{H}_d) + e^{-r(\theta_1-t)}Y_{\theta_1}W_A(0,S_{\theta_1})\Bigg].$$

By plugging the expression for $W_A(0,1)$ into the right hand side and using the Markov property, one gets

$$W_A(t,S) = E_t^{(t,S,1)}\Bigg[\Bigg(\sum_{\zeta_i\le\theta_1} e^{-r(\zeta_i-t)}Y_{\zeta_i-}R + \sum_{\tau_i\le\theta_1} e^{-r(\tau_i-t)}Y_{\tau_i-}Rv_{\tau_i-}$$
$$+ \sum_{\eta_i\le\theta_1} e^{-r(\eta_i-t)}Y_{\eta_i-}(Rv_{\eta_i-}+1-\mathcal{H}_d)\Bigg)$$
$$+ e^{-r(\theta_1-t)}Y_{\theta_1}E_{\theta_1}^{(v_{\theta_1},S_{\theta_1},Y_{\theta_1})}\Bigg[\sum_{\theta_1<\zeta_i\le\theta_2} e^{-r(\zeta_i-\theta_1)}\frac{Y_{\zeta_i-}}{Y_{\eta_i}}R + \sum_{\theta_1<\tau_i\le\theta_2} e^{-r(\tau_i-\theta_1)}\frac{Y_{\tau_i-}}{Y_{\theta_1}}Rv_{\eta_i-}$$
$$+ \sum_{\theta_1<\eta_i\le\theta_2} e^{-r(\eta_i-\theta_1)}\frac{Y_{\eta_i-}}{Y_{\theta_1}}(Rv_{\eta_i-}+1-\mathcal{H}_d) + e^{-r(\theta_2-\theta_1)}\frac{Y_{\theta_2}}{Y_{\theta_1}}W_A(v_{\theta_2},S_{\theta_2})\Bigg].$$

Thus,

$$W_A(t,S)$$
$$= E_t^{(t,S,1)}\Bigg[\Bigg(\sum_{\zeta_i\le\theta_2} e^{-r(\zeta_i-t)}Y_{\zeta_i-}R + \sum_{\tau_i\le\theta_2} e^{-r(\tau_i-t)}Y_{\tau_i-}Rv_{\tau_i-}$$
$$+ \sum_{\eta_i\le\theta_2} e^{-r(\eta_i-t)}Y_{\eta_i-}(Rv_{\eta_i-}+1-\mathcal{H}_d) + e^{-r(\theta_2-t)}Y_{\theta_2}W_A(v_{\theta_2},S_{\theta_2})\Bigg)\Bigg].$$

Repeating this for N times, we get

$$W_A(t,S) = E_t^{(t,S,1)}\Bigg[\sum_{t\le\zeta_i\le\theta_N} e^{-r(\zeta_i-t)}Y_{\zeta_i-}R + \sum_{t\le\tau_i\le\theta_N} e^{-r(\tau_i-t)}Y_{\tau_i-}Rv_{\tau_i-}$$
$$+ \sum_{t\le\eta_i\le\theta_N} e^{-r(\eta_i-t)}Y_{\eta_i-}(Rv_{\eta_i-}+1-\mathcal{H}_d) + e^{-r(\theta_N-t)}Y_{\theta_N}W_A(v_{\theta_N},S_{\theta_N})\Bigg], \tag{24}$$

where θ_N denotes the N-th coupon payment time. Thanks to the boundedness of W_A, we have

$$0 \le \lim_{N\to\infty} E_t^{(t,S,1)}\left[e^{-r(\theta_N-t)}Y_{\theta_N}W_A(v_{\theta_N},S_{\theta_N})\right]$$
$$\le \overline{K}\cdot\lim_{N\to\infty} E_t^{(t,S,1)}\left[e^{-r(\theta_N-t)}\right] = 0.$$

Here, to see the last equality, it suffices to note that (1) for two consecutive regular payouts ζ_i, ζ_{i+1}, we have $\zeta_{i+1}-\zeta_i \ge T$, therefore $E_t^{t,S,1}\left[e^{-r(\zeta_{i+1}-\zeta_i)}\right] \le e^{-rT} := K_1 < 1$; (2) for two consecutive upward

resets τ_i, τ_{i+1}, we have $E_t^{t,S,1}\left[e^{-r(\tau_{i+1}-\tau_i)}\right] = E_0^{0,1,1}\left[e^{-r\tau_1}\right] := K_2 < 1$; (3) for two consecutive downward resets η_i, η_{i+1}, we have $E_t^{t,S,1}\left[e^{-r(\eta_{i+1}-\eta_i)}\right] = E_0^{0,1,1}\left[e^{-r\eta_1}\right] := K_3 < 1$. Consequently, for $k \geq 1$, we have

$$E_t^{t,S,1}\left[e^{-r(\theta_{3k+3}-\theta_{3k})}\right] \leq K_1 \wedge K_2 \wedge K_3 < 1,$$

since there must be two regular payouts, upward resets or downward resets in $\theta_{3k}, \ldots, \theta_{3k+3}$. Therefore,

$$E_t^{t,S,1}\left[e^{-r(\theta_{3k+3}-t)}\right] \leq e^{rt} \cdot (K_1 \wedge K_2 \wedge K_3)^k \to 0, \text{ as } k \to \infty,$$

and the claim follows from the monotonicity of (θ_k). Therefore, by sending $N \to \infty$, we infer that the right hand side of (24) converges to (23). This shows that any W_A is equal to the right hand side of (23), which gives the uniqueness of W_A satisfying (22).

THEOREM 5. *W_A is the unique classical solution*[16] *to the following partial differential equation on* $\{(t,S) : 0 \leq t < T, H_d(t) < S < H_u(t)\}$

$$-\frac{\partial W_A}{\partial t} = \frac{1}{2}\sigma^2 S^2 \frac{\partial^2 W_A}{\partial S^2} + rS\frac{\partial W_A}{\partial S} - rW_A, \qquad 0 \leq t < T, H_d(t) < S < H_u(t) \tag{25}$$

$$W_A(T,S) = RT + W_A(0, S - \frac{\alpha}{1+\alpha}RT), \qquad H_d(T) < S < H_u(T) \tag{26}$$

$$W_A(t, H_u(t)) = Rt + W_A(0,1), \qquad 0 \leq t \leq T \tag{27}$$

$$W_A(t, H_d(t)) = Rt + 1 - \mathcal{H}_d + \mathcal{H}_d W_A(0,1), \qquad 0 \leq t \leq T. \tag{28}$$

Proof of Theorem 5. Proposition 1 shows that we can rewrite (22) in a non-recursive form as

$$W_A(t,S) = E_t^{(t,S,1)}\left[\sum_{\zeta_i \geq t} e^{-r(\zeta_i - t)} Y_{\zeta_i -} RT + \sum_{\tau_i \geq t} e^{-r(\tau_i - t)} Y_{\tau_i -} R v_{\tau_i -} + \sum_{\eta_i \geq t} e^{-r(\eta_i - t)} Y_{\eta_i -}(R v_{\eta_i -} + 1 - \mathcal{H}_d)\right],$$

where $E_t^{(u,s,y)}$ is the $\mathbb{Q}$-expectation computed under the initial condition $v_{t-} = u$, $S_{t-} = s$, and $Y_{t-} = y$. So it remains to show that W_A given as (23) is the unique classical solution to (8) – (11). We prove this result based on the stochastic representation result for nonlocal PDE, i.e. Corollary 3.1 in Dai et al. (2017), and in the following we first establish a connection between this theorem and (1).

We first transform S_t to a process $X_t \in [0,1]$:

$$X_t = \Gamma(v_t, S_t) = \frac{S_t - H_d(v_t)}{H_u(v_t) - H_d(v_t)}.$$

[16] By classical solution we mean $W_A \in C^{1,2}(Q) \cap C(\overline{Q} \backslash D)$, where $Q = \{(t,S) : 0 \leq t < T, H_d(t) < S < H_u(t)\}$ and $D = \{T\} \times \{H_d(T), H_u(T)\}$.

For X, the lower and upper limit becomes 0 and 1, respectively. X can be interpreted as the relative distance of S to the lower limit H_d in $[H_d(t), H_u(t)]$. Under this transform, by Ito's formula, we have

$$dX_s = b(v_s, X_s)ds + \sigma(v_s, X_s)d\mathcal{B}_s,$$

where

$$\begin{aligned} b(v,x) &= r(x-1) - \frac{\alpha}{1+\alpha}\frac{R}{H_u(t)-H_d(t)} + \frac{rH_u(t)}{H_u(t)-H_d(t)}, \\ \sigma(v,x) &= \sigma\left(\frac{H_u(t)}{H_u(t)-H_d(t)} + x - 1\right). \end{aligned}$$

Besides, after this transform, the definition τ_i, η_i and ζ_i becomes

$$\begin{aligned} &\tau_i = \inf\{s > \tau_{i-1} : X_{s-} \geq 1\}, \eta_i = \inf\{s > \eta_{i-1} : X_{s-} \leq 0\} \\ &\zeta_i = \inf\{s > \zeta_{i-1} : v_{s-} = T, X_{s-} \in (0,1)\}. \end{aligned}$$

On these dates, the change of X is described as

$$X_{\zeta_i} = X_{\zeta_i -}, X_{\tau_i} = X_{\eta_i} = \frac{1 - H_d(0)}{H_u(0) - H_d(0)},$$

and on η_i, we have

$$Y_{\eta_i} = \mathcal{H}_d Y_{\eta_i -},$$

due to the reduction in the number of shares.

Now denote $\mathcal{O} = (0,1)$,

$$\begin{aligned} g(x) &= \frac{1 - H_d(0)}{H_u(0) - H_d(0)} \cdot \mathbf{1}_{x=0,1}(x) + x \cdot \mathbf{1}_{x\in(0,1)}(x) \\ \tilde{\nu}_{t,x} &= \delta_{0,g(x)}(ds, dz) \\ \bar{\nu}(t,x) &= \mathcal{H}_d \cdot \mathbf{1}_{x=0}(x) + 1_{0<x\leq 1}(x) \\ \theta_i &= \inf\{s > \theta_{i-1} : X_{s-} = 0 \text{ or } X_{s-} = 1 \text{ or } v_{s-} = T\} \\ x &= \Gamma(t, S) \\ \tilde{W}_A(t,x) &= W_A(t,S). \end{aligned}$$

Also, the payouts of Class A coins at regular payout or reset dates can be expressed as $\tilde{h}(v_{\theta_i -}, X_{\theta_i -}, \bar{\nu}(X_{\theta_i -}))$, where $\tilde{h}(v,x,u) = 1 - u + Rv$. Using the above definitions, W_A defined in (23) can be expressed as

$$\tilde{W}_A(t,x) = E_t^x\left[\sum_{\theta_i \geq t} e^{-r(\theta_i - t)} Y_{\theta_i -} \tilde{h}(v_{\theta_i -}, X_{\theta_i -}, \bar{\nu}(X_{\theta_i -}))\right].$$

where E_t^x means the expectation calculated under $X_{t-}=x$, $v_{t-}=t$ and $Y_{t-}=1$. Then, Corollary 3.1 in Dai et al. (2017) shows that $\tilde{W}_A$ is the unique classic solution to

$$-\frac{\partial \tilde{W}_A}{\partial t}-\frac{1}{2}\sigma^2(t,x)\frac{\partial^2 \tilde{W}_A}{\partial x^2}-b(t,x)\frac{\partial \tilde{W}_A}{\partial x}=0 \qquad \text{in } [0,T)\times(0,1) \tag{29}$$

$$\tilde{W}_A(T,x)=RT+\tilde{W}_A(0,g(x)) \qquad \text{in } (0,1) \tag{30}$$

$$\tilde{W}_A(t,0)=1-\bar{\nu}(0)+Rt+\bar{\nu}(0)\tilde{W}_A(0,g(0)) \qquad \text{on } [0,T] \tag{31}$$

$$\tilde{W}_A(t,1)=Rt+\tilde{W}_A(0,g(1)) \qquad \text{on } [0,T]. \tag{32}$$

By reverting the transform $(t,s)\mapsto(t,x)=\left(t,\frac{s-H_d(t)}{H_u(t)-H_d(t)}\right)$, we conclude that W_A defined in (22) is the unique classical solution to (8) – (11).

F. Proof of Theorem 4

We follow the notations in Section E. From the proof of Theorem 5, it suffices to consider the sequence $(\tilde{W}_A^{(k)})$ defined via the transformed equation (29) – (32) by iteration with $\tilde{W}_A^{(0)}=0$. Indeed, once we show that $(\tilde{W}_A^{(k)})$ converges uniformly to $\tilde{W}_A$, by reverting the transform $(t,s)\mapsto(t,x)=\left(t,\frac{s-H_d(t)}{H_u(t)-H_d(t)}\right)$, we have that $(W_A^{(k)})$ also converges uniformly to W_A, which establishes the theorem. We shall do it in the following two steps.

Step I. First, we show that the solution $\tilde{W}_A^{(k)}(t,x)$ can be stochastically represented as

$$\tilde{W}_A^{(k)}(t,x)=E_t^x\left[\sum_{t\le\theta_i\le\theta_k} e^{-r(\theta_i-t)}Y_{\theta_i-}\tilde{h}(v_{\theta_i-},X_{\theta_i-},\bar{\nu}(X_{\theta_i-}))\right].$$

Indeed, for $k=1$, by Feynman-Kac representation for diffusion processes, the equation

$$\begin{aligned}
-\frac{\partial \tilde{W}_A}{\partial t}=&\frac{1}{2}\sigma^2(t,x)\frac{\partial^2 \tilde{W}_A}{\partial x^2}+b(t,x)\frac{\partial \tilde{W}_A}{\partial x}-r\tilde{W}_A && 0\le t<T, 0<x<1\\
\tilde{W}_A(T,x)=&RT && 0<x<1\\
\tilde{W}_A(t,1)=&Rt && 0\le t\le T\\
\tilde{W}_A(t,0)=&Rt+1-\mathcal{H}_d && 0\le t\le T.
\end{aligned}$$

has a unique classical solution $\tilde{W}_A^{(1)}\in C^{1,2}(Q)\cap C(\overline{Q}\backslash D)$, which can be represented as

$$\tilde{W}_A^{(1)}(t,x)=E_t^x\left[e^{-r(\theta_1-t)}Y_{\theta_1-}\tilde{h}(v_{\theta_1-},X_{\theta_1-},\bar{\nu}(X_{\theta_1-}))\right].$$

This establishes the claim for $k=1$. Now assume that this claim has been established for $k=i$, $i>1$. Then we have

$$E_t^x\left[\sum_{t\le\theta_j\le\theta_{i+1}} e^{-r(\theta_j-t)}Y_{\theta_j-}\tilde{h}(v_{\theta_j-},X_{\theta_j-},\bar{\nu}(X_{\theta_j-}))\right]$$

$$
\begin{aligned}
&= E_t^x\left[e^{-r(\theta_1-t)}Y_{\theta_1-}\tilde{h}(v_{\theta_1-},X_{\theta_1-},\bar{\nu}(X_{\theta_1-}))\right]\\
&\quad + E_t^x\left[e^{-r(\theta_1-t)}E_{\theta_1}^{v_{\theta_1},X_{\theta_1},Y_{\theta_1}}\left[\sum_{\theta_1<\theta_j\le\theta_{i+1}} e^{-r(\theta_j-\theta_1)}Y_{\theta_j-}\tilde{h}(v_{\theta_j-},X_{\theta_j-},\bar{\nu}(X_{\theta_j-}))\right]\right]\\
&= E_t^x\left[e^{-r(\theta_1-t)}Y_{\theta_1-}\tilde{h}(v_{\theta_1-},X_{\theta_1-},\bar{\nu}(X_{\theta_1-})) + e^{-r(\theta_1-t)}Y_{\theta_1}\tilde{W}_A^{(i)}(v_{\theta_1},X_{\theta_1})\right],
\end{aligned}
$$

where the last equality is from the Markov property and time-homogeneity of (v,X,Y). On the other hand, from the Feynman-Kac representation, the equation

$$
\begin{aligned}
-\frac{\partial\tilde{W}_A}{\partial t} =& \frac{1}{2}\sigma^2(t,x)\frac{\partial^2\tilde{W}_A}{\partial x^2} + b(t,x)\frac{\partial\tilde{W}_A}{\partial x} - r\tilde{W}_A && 0\le t<T, 0<x<1\\
\tilde{W}_A(T,x) =& RT + \tilde{W}_A^{(i)}(0,g(x)) && 0<x<1\\
\tilde{W}_A(t,1) =& Rt + \tilde{W}_A^{(i)}(0,g(1)) && 0\le t\le T\\
\tilde{W}_A(t,0) =& Rt + 1 - \mathcal{H}_d + \mathcal{H}_d\tilde{W}_A^{(i)}(0,g(0)) && 0\le t\le T.
\end{aligned}
$$

has a unique classical solution, $\tilde{W}_A^{(i+1)}$, which can be represented as

$$
\begin{aligned}
\tilde{W}_A^{(i+1)}(t,x) = E_t^x\Bigg[& e^{-r(\theta_1-t)}Y_{\theta_1-}\tilde{h}(v_{\theta_1-},X_{\theta_1-},\bar{\nu}(X_{\theta_1-}))\\
&+ e^{-r(\theta_1-t)}Y_{\theta_1}\tilde{W}_A^{(i)}(v_{\theta_1},X_{\theta_1})\Bigg].
\end{aligned}
$$

Therefore,

$$
\tilde{W}_A^{(i+1)}(t,x) = E_t^x\left[\sum_{t\le\theta_j\le\theta_{i+1}} e^{-r(\theta_j-t)}Y_{\theta_j-}\tilde{h}(v_{\theta_j-},X_{\theta_j-},\bar{\nu}(X_{\theta_j-}))\right],
$$

and the claim is proved by induction.

Step II. Next we prove the uniform convergence of $(\tilde{W}_A^{(k)})$ to $\tilde{W}_A$. To see this,

$$
\begin{aligned}
&|\tilde{W}_A^{(k)}(t,x) - \tilde{W}_A(t,x)|\\
&= \left|E_t^x\left[e^{-r(\theta_k-t)}\sum_{\theta_j>\theta_k} e^{-r(\theta_j-\theta_k)}Y_{\theta_j-}\tilde{h}(v_{\theta_j-},X_{\theta_j-},\bar{\nu}(X_{\theta_j-}))\right]\right|\\
&\le \bar{K}\cdot\sup_{(t,x)\in[0,T)\times(0,1)} E_t^x\left[e^{-r(\theta_k-t)}\right],
\end{aligned}
$$

where $\bar{K}$ is as defined in the proof of Proposition 1.

We claim that the right hand side converges to 0. Suppose this claim is proved, we then have the uniform convergence of $(\tilde{W}_A^{(k)})$ in $[0,T)\times(0,1)$. Using the terminal and boundary conditions of the equation for $\tilde{W}_A^{(k)}$, $(\tilde{W}_A^{(k)})$ also converges uniformly on $[0,T]\times[0,1]$.

To verify the claim, it suffices to note that (1) for two consecutive regular payouts ζ_i,ζ_{i+1}, we have $\zeta_{i+1}-\zeta_i\ge T$, therefore $E_t^x\left[e^{-r(\zeta_{i+1}-\zeta_i)}\right]\le e^{-rT} := K_1 < 1$; (2) for two consecutive upward resets

τ_i, τ_{i+1}, we have $E_t^x\left[e^{-r(\tau_{i+1}-\tau_i)}\right] = E_0^{g(1)}\left[e^{-r\tau_1}\right] := K_2 < 1$; (3) for two consecutive downward resets η_i, η_{i+1}, we have $E_t^x\left[e^{-r(\eta_{i+1}-\eta_i)}\right] = E_0^{g(0)}\left[e^{-r\eta_1}\right] := K_3 < 1$. Consequently, for $k \geq 1$, we have

$$E_t^x\left[e^{-r(\theta_{3k+3}-\theta_{3k})}\right] \leq K_1 \wedge K_2 \wedge K_3 < 1,$$

since there must be two consecutive regular payouts, upward resets or downward resets in $\theta_{3k}, \ldots, \theta_{3k+3}$. Therefore,

$$\sup_{(t,x)\in[0,T)\times(0,1)} E_t^x\left[e^{-r(\theta_{3k+3}-t)}\right] \leq e^{rt} \cdot (K_1 \wedge K_2 \wedge K_3)^k \to 0, \text{ as } k \to \infty,$$

and the claim follows from the monotonicity of (θ_k).